

UN  
82  
P343b  
2004

**BINDING STUDIES OF 2-ACETYLNAPHTHALENE WITH NATIVE AND  
METHYLATED CYCLODEXTRINS USING FLUORESCENCE SPECTROSCOPY**

**THE USE OF GAS CHROMATOGRAPHY/MASS SPECTROPHOTOMETRY TO  
ANALYZE ORGANIC CONTAMINANTS IN LOCAL WATERS**

By

Amy L. Payeur

\*\*\*\*\*

Submitted in partial fulfillment  
of the requirements for  
Honors in the Department of Chemistry

UNION COLLEGE

June, 2004

### ABSTRACT

PAYEUR, A.L. Binding studies of 2-Acetylnaphthalene with native and methylated cyclodextrins using fluorescence spectroscopy. Department of Chemistry, June 2004.

The main goal of this work was to explore complexes formed between 2-acetylnaphthalene (2-AN) and unsubstituted  $\alpha$ ,  $\beta$ , and  $\gamma$ -cyclodextrins as well as 2-AN and methylated  $\alpha$ ,  $\beta$  and  $\gamma$ -cyclodextrins. The substituted cyclodextrins used were trimethyl- $\alpha$ -cyclodextrin (TM- $\alpha$ -CD), trimethyl- $\beta$ -cyclodextrin (TM- $\beta$ -CD), trimethyl- $\gamma$ -cyclodextrin (TM- $\gamma$ -CD), and dimethyl- $\beta$ -cyclodextrin (DM- $\beta$ -CD). For the trimethylated cyclodextrins, all three of the -OH groups on the cyclodextrin ring are replaced by -OCH<sub>3</sub> groups. The dimethylated cyclodextrin on the other hand only has 18 of the 21 -OH groups replaced by -OCH<sub>3</sub> groups. Binding constants were determined for complexes using fluorescence quenching experiments at varying temperatures. Thermodynamic parameters of complex formation ( $\Delta H^\circ$  and  $\Delta S^\circ$ ) were determined for 2-AN with DM- $\beta$ -CD. Most of the CD's form a 1:1 complex with 2-AN but 1:2 (2-AN:(TM- $\alpha$ -CD)<sub>2</sub>) and 2:2 complexes are also observed, and no complex is observed for 2-AN with TM- $\gamma$ -CD.

### ABSTRACT

PAYEUR, A.L. The use of gas chromatography/mass spectrophotometry to analyze organic contaminants in local waters. Department of Chemistry, June 2004

The chemistry department has recently obtained a new Gas Chromatograph/Mass Spectrophotometer (GC/MS) which can be used to identify and determine quantitatively small quantities of organic contaminants. We want to use the GC/MS to analyze for organic contaminants in local waters such as the Hans Groot Kill and other nearby streams. We began by preparing a standard containing a number of organics (toluene, naphthalene, dodecane, ethylbenzene, phenol) that may be found in gasoline. We used this standard to determine the detection limits and response linearity for each of the analytes using the instrument. The ultimate goal of this project was to introduce a new method into the laboratory component of the Quantitative Analysis course, which features an ongoing project involving the analysis of local waters.

## ACKNOWLEDGEMENTS

Thank you to the entire Union College Chemistry Department for an amazing undergraduate experience. There are few places in the world where one can learn so much while having so much fun. Meg and Kathy, thank you for helping to keep this amazing department running so smoothly.

Thank you, Professor Hagerman, for introducing me to the world of research. Your guidance and friendship, both in and out of the lab, have had a profound effect on my career and will never be forgotten.

Bob Herbst, thank you for introducing me to Mike, helping me in the lab and for being an absolutely amazing friend. Union Chemistry would have never been the same without you. Also, thank you, Mark Kostuk, for your patience, assistance and entertainment my first summer in the Hagerman Group.

Professor Werner, thank you for always expecting a lot out of me, always pushing my limits and always having faith in me. Words cannot express my appreciation for your endless patience and guidance over the past four years; it has been a pleasure.

Jamie Iannacone, thank you for your previous work on this project and many thanks for your amazing notes, they made learning the ropes much easier.

Thank you Professors Kehlbeck and Schnabel for not only being excellent professors but for also being wonderful friends. Your lessons both in and out of the classroom are irreplaceable.

Kristin Bonomo and Christopher Rill, thank you for being the most supportive and encouraging people in my life. It can be very difficult to love a chemistry major as unconditionally as you two have and I am forever grateful. Therefore, too you both, I dedicate this work.

Finally, I would like to thank my parents who, after four years, understand that publications are good and that, yes, I will be getting paid to go to grad school. The past four years would not have been possible without them.

## TABLE OF CONTENTS

|   |     |
|---|-----|
| Abstract  | ii  |
| Abstract  | iii |
| Acknowledgments   | iv  |
| Table of Figures  | vii |
| Table of Tables   | ix  |
| Part I.   |     |
| Introduction  | 2   |
| Experimental  |     |
| A. Instrumentation and Chemicals Used   | 6   |
| B. The Binding Constant of 2-AN with DM- $\beta$ -CD  | 6   |
| C. The Binding Constant of 2-AN with TM- $\alpha$ -CD   | 7   |
| D. 2-AN with $\alpha$ -CD in the Presence of a Fixed<br>Concentration of TM- $\alpha$ -CD                       | 9   |
| E. 2-AN with TM- $\gamma$ -CD   |     |
| F. 2-AN with TM- $\alpha$ -CD and DM- $\beta$ -CD   | 12  |
| G. 2-AN with TM- $\beta$ -CD and DM- $\beta$ -CD  | 13  |
| Results   |     |
| A. The Binding of 2-AN to DM- $\beta$ -CD   | 14  |
| B. The Binding of 2-AN and TM- $\alpha$ -CD   | 19  |
| C. Binding of 2-AN with a Fixed Concentration of TM- $\alpha$ -CD<br>and Varying Concentrations of $\alpha$ -CD | 25  |
| D. Fluorescence Intensity of 2-AN in the Presence of TM- $\gamma$ -CD   | 28  |
| E. The Binding of 2-AN to TM- $\alpha$ -CD and DM- $\beta$ -CD  | 30  |
| F. The Binding of 2-AN to TM- $\beta$ -CD and DM- $\beta$ -CD   | 30  |

|  |           |
|--|-----------|
| <b>Discussion</b>  |           |
| <b>A. The Binding of 2-AN with DM-<math>\beta</math>-CD</b>    | <b>31</b> |
| <b>B. The Binding of 2-AN with Permethylated Cyclodextrins</b> | <b>32</b> |
| <b>C. The Binding of 2-AN in Cyclodextrin Mixtures</b>         | <b>34</b> |
| <b>References</b>  | <b>36</b> |
| <br>   |           |
| <b>Part II.</b>  |           |
| <b>Introduction</b>  | <b>38</b> |
| <b>Experimental</b>  | <b>39</b> |
| <b>Results</b>   | <b>42</b> |
| <b>Discussion</b>  | <b>63</b> |
| <b>References</b>  | <b>65</b> |

## TABLE OF FIGURES

### Part I.

|   |    |
|---|----|
| Figure 1. $\alpha$ -CD, $\beta$ -CD and $\gamma$ -CD  | 2  |
| Figure 2. Torroidal shape of cyclodextrins  | 3  |
| Figure 3. 2-Acetylnaphthalene   | 4  |
| Figure 4. 2-AN with DM- $\beta$ -CD at 25.0 °C  | 15 |
| Figure 5. Modified Stern-Volmer Plot for 2-AN with DM- $\beta$ -CD at 25 °C                 | 16 |
| Figure 6. Van't Hoff plot for 2-AN with DM- $\beta$ -CD                                     | 18 |
| Figures 7. Fluorescence spectrum of 2-AN with TM- $\alpha$ -CD                              | 21 |
| Figure 8. Stern-Volmer plot of 2-AN with TM- $\alpha$ -CD at 24 °C                          | 22 |
| Figure 9. Stern-Volmer plot of 2-AN with TM- $\alpha$ -CD at 24 °C                          | 23 |
| Figure 10. 2-AN with TM- $\alpha$ -CD with SDAS at 24 °C                                    | 24 |
| Figure 11. Modified Stern-Volmer plot of 2-AN with TM- $\alpha$ -CD and $\alpha$ -CD        | 26 |
| Figure 12. Quenching data for 2-AN with TM- $\alpha$ -CD, $\alpha$ -CD and TM- $\alpha$ -CD | 27 |
| Figure 13. 2-AN with TM- $\gamma$ -CD at 25 °C  | 29 |

### Part II.

|   |    |
|---|----|
| Figure 1. Gas chromatogram of stock                                   | 45 |
| Figure 2. Gas chromatogram of stock and mass spectrum of toluene      | 46 |
| Figure 3. Gas chromatogram of stock and mass spectrum of phenol       | 47 |
| Figure 4. Gas chromatogram of stock and mass spectrum of acetophenone | 48 |
| Figure 5. Gas chromatogram of stock and mass spectrum of naphthalene  | 49 |

|   |    |
|---|----|
| Figure 6. Gas chromatogram of stock and mass spectrum of dodecane   | 50 |
| Figure 7. Average peak height vs. toluene concentration for 1 $\mu$ L, 2 $\mu$ L and 5 $\mu$ L injection sizes      | 51 |
| Figure 8. Average peak height vs. phenol concentration for 1 $\mu$ L, 2 $\mu$ L and 5 $\mu$ L injection sizes       | 52 |
| Figure 9. Average peak height vs. acetophenone concentration for 1 $\mu$ L, 2 $\mu$ L and 5 $\mu$ L injection sizes | 53 |
| Figure 10. Average peak height vs. naphthalene concentration for 1 $\mu$ L, 2 $\mu$ L and 5 $\mu$ L injection sizes | 54 |
| Figure 11. Average peak height vs. dodecane concentration for 1 $\mu$ L, 2 $\mu$ L and 5 $\mu$ L injection sizes    | 55 |
| Figure 12. Gas chromatogram of 10 ppm toluene, phenol, and acetophenone solution                                    | 56 |
| Figure 13. Gas chromatogram of 2 ppm toluene and acetophenone solution  | 57 |
| Figure 14. Gas chromatogram of solutions with 80 ppb toluene and acetophenone                                       | 58 |
| Figure 15. Gas chromatogram of 40 ppb toluene and acetophenone solutions  | 59 |
| Figure 16. Gas chromatogram of Patroon sample, run 1  | 60 |
| Figure 17. Gas chromatogram of Patroon sample   | 61 |
| Figure 18. Gas chromatogram of Hans Groot Kill sample   | 62 |



## TABLE OF TABLES

### Part I.

|  |    |
|--|----|
| Table 1. Solutions of 2-An with DM- $\beta$ -CD in water                       | 6  |
| Table 2. Temperatures used in Trials 1-5                                       | 7  |
| Table 3. Solutions of 2-AN with TM- $\alpha$ -CD in water                      | 8  |
| Table 4. 5mL solutions of 2-AN with TM- $\alpha$ -CD in water                  | 9  |
| Table 5. Solutions of 2-AN with $\alpha$ -CD in water                          | 10 |
| Table 6. Solutions of 2-AN with TM- $\alpha$ -CD and $\alpha$ -CD in water     | 11 |
| Table 7. Solutions of 2-AN with TM- $\gamma$ -CD in water                      | 11 |
| Table 8. Solutions of 2-AN with TM- $\alpha$ -CD and DM- $\beta$ -CD in water  | 12 |
| Table 9. Solutions of 2-AN with TM- $\beta$ -CD and DM- $\beta$ -CD in water   | 13 |
| Table 10. 2-AN with DM- $\beta$ -CD binding constant summary data              | 14 |
| Table 11. 2-AN with TM- $\alpha$ -CD K values when fit with Excel and SDAS     | 20 |
| Table 12. 2-AN with TM- $\alpha$ -CD and DM- $\beta$ -CD data summary          | 30 |
| Table 13. 2-AN with TM- $\beta$ -CD and DM- $\beta$ -CD data summary           | 30 |
| Table 14. Summary of binding constants for native and methylated cyclodextrins | 31 |

### Part II.

|  |    |
|--|----|
| Table 1. Preparation of stock solution                     | 39 |
| Table 2. Serial dilutions                                  | 39 |
| Table 3. Concentration of each component for all dilutions | 40 |
| Table 4. Concentration of solution F dilutions             | 40 |

**Part I.**  
**Binding studies of 2-acetylnaphthalene with native and methylated cyclodextrins using  
fluorescence spectroscopy**

## INTRODUCTION

Cyclodextrins are toroidal in shape and are composed of a ring of glucopyranose units. There are three types of unsubstituted cyclodextrins: alpha ( $\alpha$ ), beta ( $\beta$ ) and gamma ( $\gamma$ ).  $\alpha$ -CD is composed of six glucopyranose units,  $\beta$ -CD is composed of seven, and  $\gamma$ -CD has eight glucopyranose units (see Figure 1).

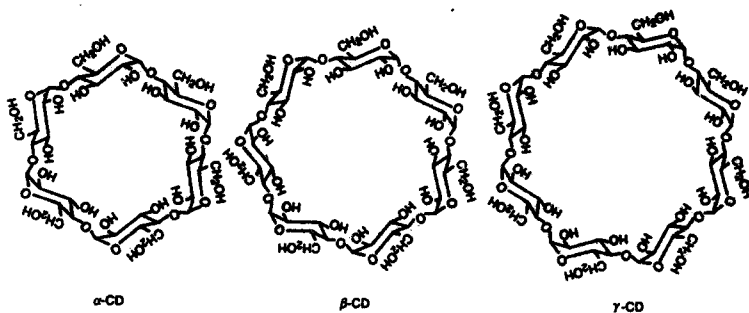
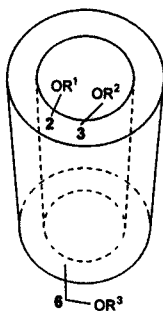


Figure 1.  $\alpha$ -CD,  $\beta$ -CD and  $\gamma$ -CD

The inner, hydrophobic cavity of the CD's range from 0.57-0.95 nm in diameter<sup>2</sup> and each glucose unit has three -OH groups located in the 2, 3, and 6 positions. The -OH groups in the 2 and the 3 position have the ability to hydrogen bond with each other and therefore help to stabilize the toroidal shape (Figure 2).



**Figure 2.** Torroidal shape of cyclodextrins. Note  $\text{-OH}$ 's in 2, 3, and 6 position.

In this work, we were interested in two types of methylated CD's. The first is a dimethyl (DM) cyclodextrin, in which the  $\text{-OH}$  groups at the 3 and the 6 position are replaced by  $\text{-OCH}_3$  groups. This partially interrupts the ability for the 2 and the 3 positions to hydrogen bond to each other. In the trimethyl (TM) or permethylated (PM) cyclodextrins all of the  $\text{-OH}$  groups are replaced by  $\text{-OCH}_3$  groups, and the ability of the 2 and 3 positions to hydrogen bond is lost completely. Previous work shows that the TM-CD's are more distorted than the native CD's; therefore, the torroidal shape is not preserved and the size of the inner cavity changes<sup>3-6,8</sup>.

Cyclodextrins are known for their ability to form host:guest complexes where the guest will bind within the hydrophobic inner cavity of the cyclodextrin. These host:guest complexes are significant for several reasons. The hydrophobic nature of the CD inner cavity aids in the solubility of nonpolar substances making them useful in pharmaceuticals. Cyclodextrins are used industrially to stabilize fragrances in soaps and detergents. These molecules are also important because they can help improve separation techniques. They act as modifiers of photochemical behavior, as agents to control dye

aggregation, and as separation enhancers in high-performance liquid chromatography (HPLC) and capillary electrophoresis (CE)<sup>1</sup>. Cyclodextrins often increase the fluorescence of analytes and can therefore be further helpful analytically.

The 2-acetylnaphthalene (2-AN) molecule (see Figure 3) is one of the many guests that can be accommodated by a cyclodextrin cavity.

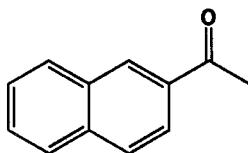


Figure 3. 2-Acetylnaphthalene (2-AN)

The formation of complexes between 2-AN and cyclodextrins can be monitored using fluorescence spectroscopy. Often, cyclodextrins increase the fluorescence of an organic fluorophore; however, in the case to 2-AN the fluorescence intensity is decreased; this occurs due to a static quenching mechanism<sup>7</sup>. Thermodynamic properties can also be determined by measuring the fluorescence of 2-AN at various temperatures and CD concentrations.

Previous work<sup>7</sup> shows that the binding of 2-AN to  $\alpha$ -CD and  $\beta$ -CD occurs in a 1:1 ratio. Werner et. al. reported that the binding constants of 2-AN with  $\alpha$ -CD and with  $\beta$ -CD are 38 +/-5 and 581 +/-6, respectively. Werner and coworkers have also shown that 2-AN forms a 2:2 complex with  $\gamma$ -CD in addition to a 1:1 complex<sup>1</sup>. The binding constant for the 1:1 complex was determined to be 49 +/-5. The binding constant of 2-AN with trimethyl-beta-cyclodextrin (TM- $\beta$ -CD) has also been determined previously to be 101 +/-4<sup>2</sup>.

The primary goal of this work was to investigate and compare the binding constants of 2-AN with un-substituted and methylated cyclodextrins. Fluorescence quenching experiments were performed and binding constants determined. In addition, binding constants of 2-AN with cyclodextrin mixtures were determined. The complex formation between the 2-AN and various cyclodextrins was also investigated via fluorescence quenching experiments as a function of temperature to determine thermodynamic properties of complexes.

## EXPERIMENTAL

### Instrumentation and Chemicals Used

All fluorescence measurements were completed using a PTI Quantmaster spectrofluorometer. A Hewlett-Packard 8452A diode array spectrophotometer was used for all absorbance measurements.  $\alpha$ -CD from both Aldrich and Wacker was used. TM- $\alpha$ -CD was received as a gift from Dr. Pitha and was later purchased from Trappsol (>97%). DM- $\beta$ -CD (>98%) was purchased from Fluka. TM- $\gamma$ -CD was also received as a gift from Dr. Pitha and solid 2-AN was received from Aldrich.

### The Binding Constant of 2-AN with DM- $\beta$ -CD

A stock solution of 2-AN was prepared by stirring solid 2-AN in Millipore (Trial 1-4) water overnight. For Trial 5 the 2-AN stock solution was prepared in de-ionized water. A stock solution of  $2.50 \times 10^{-3}$  M DM- $\beta$ -CD was prepared in de-ionized water. Both solutions were stored in brown bottles to avoid exposure to light sources. Five sets of solutions were prepared in 5mL volumetric flasks as described in Table 1. The absorbance of the 2-AN stock solution at 340 nm was obtained to insure that, after a 1 in 10 dilution, the 2-AN would have an absorbance value between 0.01 and 0.05, the ideal range for fluorescence.

Table 1. Solutions of 2-AN with DM- $\beta$ -CD in water (5.00mL total volumes)

| Solution | mL 2-AN Stock in H <sub>2</sub> O | mL DM- $\beta$ -CD Stock in H <sub>2</sub> O | [DM- $\beta$ -CD] M   |
|----------|-----------------------------------|--|-----------------------|
| 1        | 0.500                             | 0  | 0                     |
| 2        | 0.500                             | 0.500  | $2.50 \times 10^{-4}$ |
| 3        | 0.500                             | 1.00   | $5.00 \times 10^{-4}$ |
| 4        | 0.500                             | 2.00   | $1.00 \times 10^{-3}$ |
| 5        | 0.500                             | 3.00   | $1.50 \times 10^{-3}$ |
| 6        | 0.500                             | 4.00   | $2.00 \times 10^{-3}$ |

Fluorescence intensity measurements were performed on the solutions. The experiments were repeated five times (Trials 1-5), with a new TM- $\beta$ -CD stock solution each time. The excitation wavelength was 340 nm, the emission range was 370-550nm, the slits were 4nm and a step size of 2nm was used for Trials 1-3 and 1 nm for Trials 4-5.

The fluorescence of the six solutions was measured at four different temperatures. The temperatures used are summarized in Table 2.

**Table 2. Temperatures used in Trials 1-5**

| Trial | T <sub>1</sub> , °C | T <sub>2</sub> , °C | T <sub>3</sub> , °C | T <sub>4</sub> , °C |
|-------|---------------------|---------------------|---------------------|---------------------|
| 1     | 18.5                | 24.5                | 32.0                | 39.0                |
| 2     | 18.2                | 25.0                | 31.0                | 38.0                |
| 3     | 18.0                | 25.0                | 31.0                | 40.0                |
| 4     | 16.4                | 25.0                | 35.0                | NA                  |
| 5     | 16.5                | 25.0                | 35.0                | 43.0                |

\*All temperatures are +/- 0.1 C

\*\*T<sub>4</sub> for Trial 4 could not be obtained due to a clogged hose

An average of the K,  $\Delta H^\circ$  and  $\Delta S^\circ$  values was obtained by eliminating the data from Trials 2 and 4. These data were eliminated because they were clearly erroneous when compared to the other trials. The average values were assumed to be the K,  $\Delta H^\circ$  and  $\Delta S^\circ$  values of the complex and were used in proceeding experiments.

#### **The Binding Constant of 2-AN with TM- $\alpha$ -CD**

A  $2.5 \times 10^{-3}$  M stock solution of TM- $\alpha$ -CD was prepared in de-ionized water and stored in a brown bottle. An absorption spectrum of the 2-AN stock solution previously prepared in de-ionized water was obtained, and the absorbance at 340 nm was determined to be about 0.2; therefore, a 1 in 10 dilution was used to prepare solutions for



fluorescence quenching experiments. Solutions were prepared in 5mL volumetric flasks with de-ionized water as described in Table 3.

**Table 3. Solutions of 2-AN with TM- $\alpha$ -CD in water (5.00mL total volume)**

| Solution | mL 2-AN Stock in H <sub>2</sub> O | mL TM- $\alpha$ -CD Stock in H <sub>2</sub> O | [TM- $\alpha$ -CD] M  |
|----------|-----------------------------------|---|-----------------------|
| 1        | 0.500                             | 0   | 0                     |
| 2        | 0.500                             | 0.500   | $2.50 \times 10^{-4}$ |
| 3        | 0.500                             | 1.00  | $5.00 \times 10^{-4}$ |
| 4        | 0.500                             | 2.00  | $1.00 \times 10^{-3}$ |
| 5        | 0.500                             | 3.00  | $1.50 \times 10^{-3}$ |
| 6        | 0.500                             | 4.00  | $2.00 \times 10^{-3}$ |

Fluorescence intensity measurements were first performed, in triplicate, on all six solutions at 25 °C, using 340 nm excitation, an emission range of 370-550nm, 4nm slits, and 1 nm step size. Again, using Stern-Volmer plots, the binding constants and an average were determined. Fluorescence measurements were subsequently collected on solutions 1-6 at 16.3, 25.0, 35.0, and 43.0 °C (all temperatures +/- 0.1 °C) using the same parameters as above with the exception of the step size, which was 2nm in this case.

The Stern-Volmer plots appeared to be non-linear. It was decided to use a higher stock concentration of TM- $\alpha$ -CD to bring out the non-linearity more clearly. A  $5.0 \times 10^{-3}$  M stock solution of TM- $\alpha$ -CD was prepared in Millipore water. In addition, the absorbance of the 2-AN stock solution was increased to approximately 0.6 at 340 nm. Using this solution, a second set of solutions was prepared in 5mL volumetric flasks using Millipore water and as described in Table 4. (Prior to preparing the solutions an absorbance reading of the 2-AN stock was taken at 340nm to insure that the stock solution was prepared in the proper range for fluorescence measurements). The

fluorescence intensity was also measured for Millipore water and subtracted from the intensity of each of the solutions before graphing the Stern-Volmer plot.

**Table 4. 5mL solutions of 2-AN with TM- $\alpha$ -CD in water (5.00mL total volume)**

| Solution | mL 2-AN<br>Stock in H <sub>2</sub> O | mL TM- $\alpha$ -CD<br>Stock in H <sub>2</sub> O | [TM- $\alpha$ -CD] M  |
|----------|--------------------------------------|--|-----------------------|
| 1        | 1.00                                 | 0  | 0                     |
| 2        | 1.00                                 | 0.500  | $5.00 \times 10^{-4}$ |
| 3        | 1.00                                 | 0.750  | $7.50 \times 10^{-4}$ |
| 4        | 1.00                                 | 1.00   | $1.00 \times 10^{-3}$ |
| 5        | 1.00                                 | 1.50   | $1.50 \times 10^{-3}$ |
| 6        | 1.00                                 | 2.50   | $2.50 \times 10^{-3}$ |
| 7*       | 1.00                                 | 3.00   | $3.00 \times 10^{-3}$ |
| 8        | 1.00                                 | 3.50   | $3.50 \times 10^{-3}$ |
| 9*       | 1.00                                 | 3.75   | $3.75 \times 10^{-3}$ |
| 10       | 1.00                                 | 4.00   | $4.0 \times 10^{-3}$  |

\*only used in Trials 4 and higher

Fluorescence intensity measurements were performed using excitation at 340 nm, an emission range of 370-550nm, 4nm slits, 2nm step size and temperatures of 16.5, 24.0, 33.0, and 41.0 °C (Trial 2), 17.0, 25.0, 33.0 °C (Trial 3), 24.5 °C (Trial 4), 17.0, 24.0, 35.0, 43.5 °C (Trial 5), 18.0, 26.0 °C (Trial 6), 25.0 °C (Trial 7), 25.0 °C (Trial 8), 25.0 °C (Trial 9). All temperatures were  $\pm 0.1$  °C. Binding constants were obtained using a non-linear fit (see results).

#### **2-AN with $\alpha$ -CD in the Presence of a Fixed Concentration of TM- $\alpha$ -CD**

A 0.015 M solution of  $\alpha$ -CD was prepared in Millipore water. An absorption spectrum of the 2-AN stock solution was taken and  $A_{340} \approx 0.6$ ; therefore, after a 1 in 10 dilution it will be in the desired range. A set of six solutions was prepared as described in Table 5.

**Table 5. Solutions of 2-AN with  $\alpha$ -CD in water (10.00mL total volume)**

| Solution | mL 2-AN | mL $\alpha$ -CD | [ $\alpha$ -CD] M     |
|----------|---------|-----------------|-----------------------|
| 1        | 1.00    | 0               | 0                     |
| 2        | 1.00    | 1.8             | $2.7 \times 10^{-3}$  |
| 3        | 1.00    | 3.6             | $5.4 \times 10^{-3}$  |
| 4        | 1.00    | 5.4             | $8.1 \times 10^{-3}$  |
| 5        | 1.00    | 7.8             | $1.17 \times 10^{-2}$ |
| 6        | 1.00    | 9.0             | $1.35 \times 10^{-2}$ |

Fluorescence spectra were obtained of these six solutions with an excitation wavelength of 340 nm, and emission range of 370-550 nm, a 2 nm step size and 4 nm slits. The temperature was 25 C; a spectrum of Millipore water was also taken, the intensity of the water spectrum was subtracted from the intensity maximum of the other spectra at the wavelength of maximum intensity. These data were plotted using the modified Stern-Volmer equation (Eqn. 1).

A stock solution of  $5.0 \times 10^{-3}$  M TM- $\alpha$ -CD was prepared in Millipore water, and the solutions as described in Table 6 were then prepared. As can be seen these solutions contain a fixed concentration of TM- $\alpha$ -CD and increasing concentrations of  $\alpha$ -CD. The TM- $\alpha$ -CD concentration was chosen as the concentration beyond which the Stern-Volmer plot for 2-AN with TM- $\alpha$ -CD showed significant upward curvature.

**Table 6. Solutions of 2-AN with TM- $\alpha$ -CD and  $\alpha$ -CD in water (5.00mL total volume)**

| Solution | mL TM- $\alpha$ -CD Stock | [TM- $\alpha$ -CD] M | mL of Corresponding $\alpha$ -CD solution | [ $\alpha$ -CD] M     |
|----------|---------------------------|----------------------|---|-----------------------|
| 1        | 0.50                      | $5.0 \times 10^{-4}$ | 4.5                                       | 0.00                  |
| 2        | 0.50                      | $5.0 \times 10^{-4}$ | 4.5                                       | $2.43 \times 10^{-3}$ |
| 3        | 0.50                      | $5.0 \times 10^{-4}$ | 4.5                                       | $4.86 \times 10^{-3}$ |
| 4        | 0.50                      | $5.0 \times 10^{-4}$ | 4.5                                       | $7.29 \times 10^{-3}$ |
| 5        | 0.50                      | $5.0 \times 10^{-4}$ | 4.5                                       | $1.05 \times 10^{-2}$ |
| 6        | 0.50                      | $5.0 \times 10^{-4}$ | 4.5                                       | $1.22 \times 10^{-2}$ |

Fluorescence spectra of these solutions were taken at an excitation wavelength of 340 nm, an emission range of 370-650 nm, a 1 nm step size and 4nm slit sizes. The temperature was  $25 \pm 0.1$  °C. These data were plotted using the modified Stern-Volmer equation (Eqn. 1). The process was then repeated to ensure the reproducibility of the results.

#### 2-AN with TM- $\gamma$ -CD

A  $4.51 \times 10^{-3}$  M stock solution of TM- $\gamma$ -CD was prepared in Millipore water and used to prepare seven solutions as described in Table 7. An absorption spectrum was taken and the stock was found to have an absorbance of 0.2 at 340 nm.

**Table 7. Solutions of 2-AN with TM- $\gamma$ -CD in water (5.00mL total volume)**

| Solution | mL 2-AN Stock in H <sub>2</sub> O | mL TM- $\alpha$ -CD Stock in H <sub>2</sub> O | [TM- $\alpha$ -CD] M  |
|----------|-----------------------------------|---|-----------------------|
| 1        | 1.00                              | 0   | 0                     |
| 2        | 1.00                              | 0.55  | $5.00 \times 10^{-4}$ |
| 3        | 1.00                              | 0.83  | $7.50 \times 10^{-4}$ |
| 4        | 1.00                              | 1.1   | $1.00 \times 10^{-3}$ |
| 5        | 1.00                              | 1.7   | $1.50 \times 10^{-3}$ |
| 6        | 1.00                              | 2.8   | $2.50 \times 10^{-3}$ |
| 7        | 1.00                              | 3.9   | $3.50 \times 10^{-3}$ |

Fluorescence measurements were taken at 340 nm excitation, emission 350-670nm, 4nm slits and 2nm step size. The temperatures were 15 and 25.5 °C (both +/-0.1 °C). At both temperatures the peaks practically overlapped each other. The temperature was dropped to 10°C to see if some quenching could be obtained. At 15 °C only solutions 1-3 were run, solutions 1-4 were run at 25.5 °C and at 10 °C solutions 1-5 were run. There appeared to be no quenching of the 2-AN fluorescence at any temperature upon addition of the TM- $\gamma$ -CD.

#### 2-AN with TM- $\alpha$ -CD and DM- $\beta$ -CD

A stock solution containing both TM- $\alpha$ -CD and DM- $\beta$ -CD at a concentration of  $2.50 \times 10^{-3}$  M was prepared in de-ionized water. An absorption spectrum of 2-AN was taken and the absorbance at 340 nm was about 0.2. Six solutions were prepared in 5 mL volumetric flasks as described in Table 8 using de-ionized water.

**Table 8. Solutions of 2-AN with TM- $\alpha$ -CD and DM- $\beta$ -CD in water (5.00 mL total volume)**

| Solution | mL 2-AN<br>Stock in H <sub>2</sub> O | mL TM- $\alpha$ -CD<br>DM- $\beta$ -CD<br>Stock in H <sub>2</sub> O | [TM- $\alpha$ -CD]<br>M | [DM- $\beta$ -CD]<br>M |
|----------|--------------------------------------|---|-------------------------|------------------------|
| 1        | 0.500                                | 0   | 0                       | 0                      |
| 2        | 0.500                                | 0.500   | $2.50 \times 10^{-4}$   | $2.50 \times 10^{-4}$  |
| 3        | 0.500                                | 1.00  | $5.00 \times 10^{-4}$   | $5.00 \times 10^{-4}$  |
| 4        | 0.500                                | 2.00  | $1.00 \times 10^{-3}$   | $1.00 \times 10^{-3}$  |
| 5        | 0.500                                | 3.00  | $1.50 \times 10^{-3}$   | $1.50 \times 10^{-3}$  |
| 6        | 0.500                                | 4.00  | $2.00 \times 10^{-3}$   | $2.00 \times 10^{-3}$  |

Fluorescence quenching experiments were performed, in triplicate, at 25 °C, excitation 340nm, emission 370-550nm, 4nm slit widths and 2nm step size. Stern-Volmer plots were used to calculate K. An average of the three values was taken and was used for comparison in preceding experiments.

### 2-AN with TM- $\beta$ -CD and DM- $\beta$ -CD

A  $2.5 \times 10^{-3}$  M stock solution of both TM- $\beta$ -CD and DM- $\beta$ -CD was prepared in de-ionized water. An absorption spectrum of 2-AN was taken at 340nm and the absorbance was determined to be about 0.2. Six solutions were prepared in 5 mL volumetric flasks as described in Table 9 with de-ionized water.

**Table 9. Solutions of 2-AN with TM- $\beta$ -CD and DM- $\beta$ -CD in water (5.00mL total volume)**

| Solution | mL 2-AN<br>Stock in H <sub>2</sub> O | mL TM- $\alpha$ -CD<br>DM- $\beta$ -CD<br>Stock in H <sub>2</sub> O | [TM- $\beta$ -CD]<br>M | [DM- $\beta$ -CD]<br>M |
|----------|--------------------------------------|---|------------------------|------------------------|
| 1        | 0.500                                | 0   | 0                      | 0                      |
| 2        | 0.500                                | 0.500   | $2.50 \times 10^{-4}$  | $2.50 \times 10^{-4}$  |
| 3        | 0.500                                | 1.00  | $5.00 \times 10^{-4}$  | $5.00 \times 10^{-4}$  |
| 4        | 0.500                                | 2.00  | $1.00 \times 10^{-3}$  | $1.00 \times 10^{-3}$  |
| 5        | 0.500                                | 3.00  | $1.50 \times 10^{-3}$  | $1.50 \times 10^{-3}$  |
| 6        | 0.500                                | 4.00  | $2.00 \times 10^{-3}$  | $2.00 \times 10^{-3}$  |

Fluorescence quenching experiments were performed, in triplicate, at 25 °C, excitation 340nm, emission 370-550nm, 4nm slit widths and 2nm step size. Stern-Volmer plots were used to calculate K. Averages for the three values were obtained and used for comparison with preceding experiments.

## RESULTS

### The Binding of 2-AN to DM- $\beta$ -CD

As can be seen in Figure 4, the fluorescence intensity of 2-AN decreased as the concentration of DM- $\beta$ -CD was increased. All spectra collected throughout this work were similar to those in Figure 4. The small peak observed in the 390 nm region was Raman scatter from the solvent (water).

Binding constants were determined for each of three trials at 18, 25, 32 and, 40°C, using a modified version of the Stern-Volmer equation that assumes a 1:1 complex, Equation 1,

$$F^0/F = 1 + K[Q] \quad (1)$$

where  $F^0$  is the fluorescence intensity in the absence of quencher,  $F$  is the fluorescence intensity with quencher present,  $K$  is the binding constant and  $[Q]$  is the quencher concentration (in this case DM- $\beta$ -CD). Figure 5 is an example of a Stern-Volmer plot used to calculate the binding constants for the three trials performed. These values are summarized in Table 10.

Table 10. 2-AN with DM- $\beta$ -CD binding constant data summary

| Temp. C | K Trial 1  | K Trial 2 | K Trial 3 | Average (Stdev) |
|---------|------------|-----------|-----------|-----------------|
| 18      | 974(0.98*) | 1011(1.0) | 1020(1.0) | 1002(24)        |
| 25      | 935(0.98)  | 900(1.0)  | 917(1.0)  | 918(18)         |
| 32      | 748(0.97)  | 763(1.0)  | 731(1.0)  | 748(16)         |
| 40      | 592 (0.99) | 552(1.0)  | 497(1.0)  | 547(48)         |

\*Number in parenthesis indicates the y-intercept

At least one of the least-square fits at each temperature had an  $R^2$  value greater than 0.99. All but one of the remaining data had  $R^2$  greater than 0.98

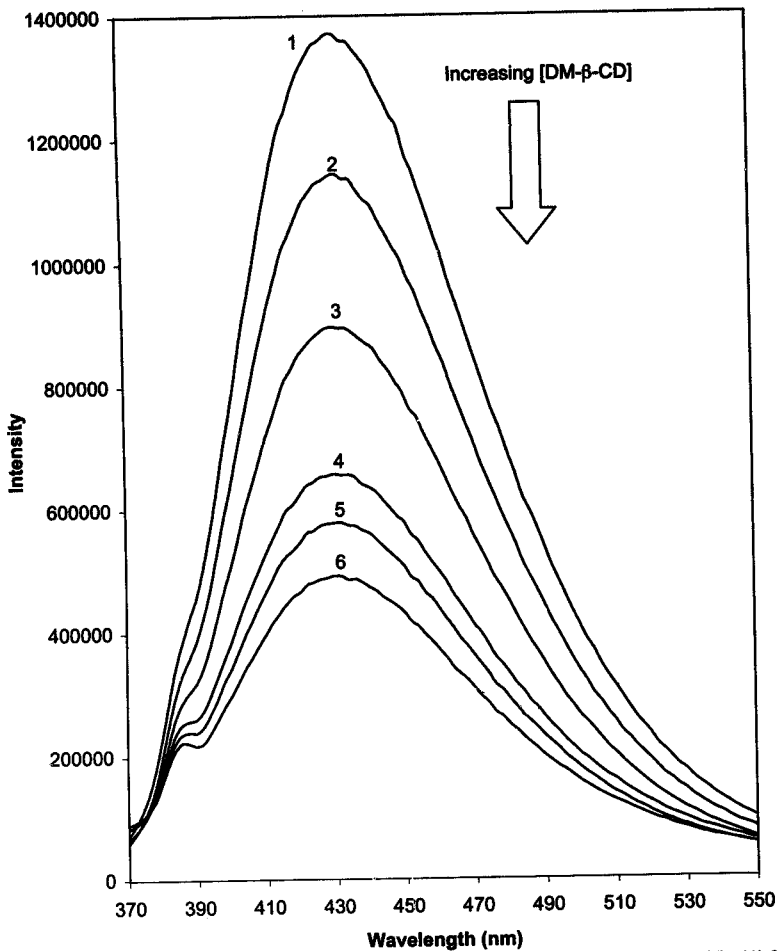


Figure 4. 2-AN with DM- $\beta$ -CD at 25.0 C. Concentrations of DM- $\beta$ -CD: (1) 0, (2)  $2.50 \times 10^{-4}$ , (3)  $5.00 \times 10^{-4}$ , (4)  $1.00 \times 10^{-3}$ , (5)  $1.50 \times 10^{-3}$ , (6)  $2.00 \times 10^{-3}$



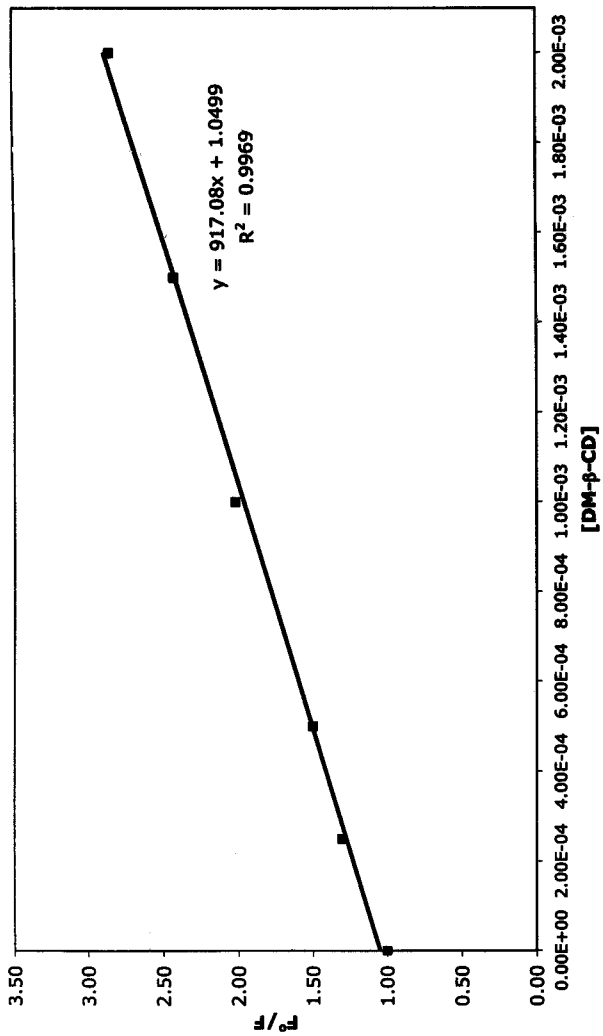


Figure 5. Modified Stern-Volmer plot for 2-AN with DM- $\beta$ -CD at 25 C

$\Delta H^\circ$  and  $\Delta S^\circ$  for the 1:1 complex formed between 2-AN and DM- $\beta$ -CD were determined through the use of a van't Hoff plot ( $\ln K$  vs  $1/T$ ) and the data from Trials 1, 3, and 5 (see Figure 6). The  $\Delta H^\circ$  and  $\Delta S^\circ$  values were determined to be  $-19.5 \pm 1.8$  kJ/mol and  $-9.3 \pm 5.9$  J/mol, respectively.

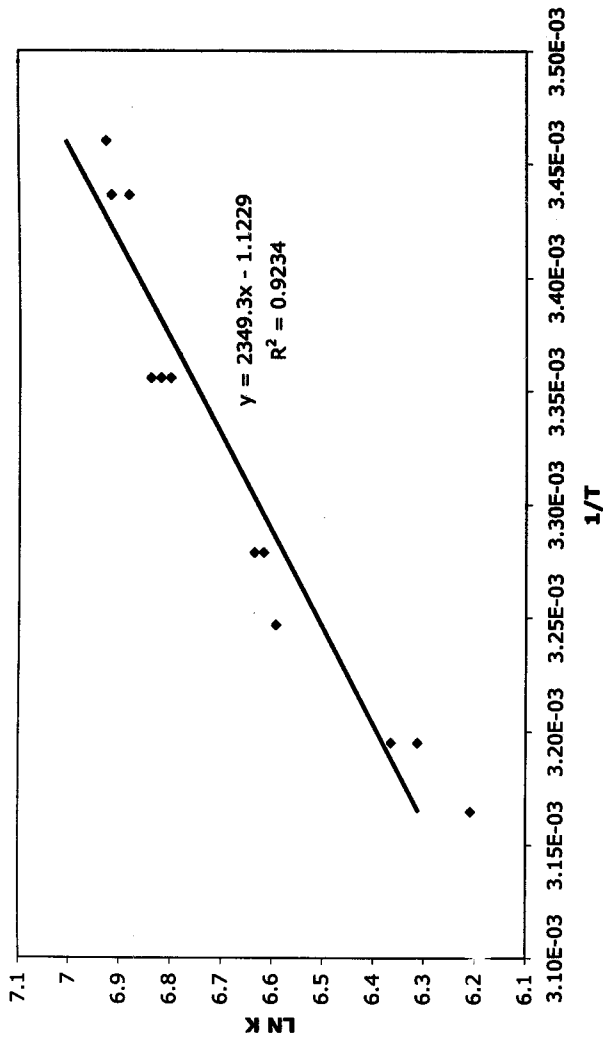


Figure 6. Van't Hoff plot for 2-AN with DM-β-CD

### The Binding of 2-AN and TM- $\alpha$ -CD

In order to obtain significant changes in fluorescence intensity, the concentration of TM- $\alpha$ -CD was increased as was the concentration of the 2-AN to decrease the effect of Raman scatter. The spectra collected after this change produced distinct intensity changes (see Figure 7). It was observed that, as with the DM- $\beta$ -CD, the fluorescence intensity decreased as the [TM- $\alpha$ -CD] increased. At all four temperatures it is obvious that the Stern-Volmer plots cannot be fit linearly (see Figure 8). Instead the data were fit to a polynomial equation based on the assumption that both a 1:1 (2-AN:TM- $\alpha$ -CD) and a 1:2 (2-AN:(TM- $\alpha$ -CD)<sub>2</sub>) complex are formed.

The variables are defined as:

A = 2-AN

CD = TM- $\alpha$ -CD

F<sup>0</sup> = fluorescence intensity without quencher

F = fluorescence intensity in the presence of quencher



A mass balance of all the A containing species and all the CD containing species gives:

$$[A]_0 = [A] + [ACD] + [A(CD)_2] \quad (4)$$

$$C_{CD} = [CD] + [ACD] + 2[A(CD)_2] = [CD] \text{ since } C_{CD} \gg [A]_0 \quad (5)$$

Substitution into Eq. 4 using Eq. 2 and Eq. 3 gives the following:

$$[A]_0 = [A] + K_1[A]C_{CD} + K_2[ACD]C_{CD} \quad (6)$$

$$[A]_0 = [A] + K_1[A]C_{CD} + K_1K_2[A]C_{CD}^2 \quad (7)$$

Rearrangement then gives Eq. 8:

$$[A]_0/[A] = 1 + K_1 C_{CD} + K_1 K_2 C_{CD}^2 \quad (8)$$

Because  $F^0 = k[A]_0$  and  $F = k[A]$  the following is true..

$$F^0/F = 1 + K_1 C_{CD} + K_1 K_2 C_{CD}^2 \quad (9)$$

Where  $K_1$  is the binding constant for a 1:1 complex and  $K_2$  is the binding constant for a 1:2 complex. The  $F^0/F$  vs.  $[CD]$  data were fit using both a second order polynomial trend line in Microsoft Excel (see Figure 9) and using Equation 2 in the Statistical Data Analysis Software Program (See Figure 10). In the SDAS program  $K_1$  was defined as  $K$  and  $K_2$  was defined as  $J$ . Table 11 is an example of the data obtained from these fits.

Average  $K$  values were obtained for all of the trials run.  $K_{1\text{average}} = 209 \pm 79$  and

$K_{2\text{average}} = 1273 \pm 49$ .

**Table 11. 2-AN with TM- $\alpha$ -CD K values when fit with Excel and SDAS**

| Temperature | $K_1$ Excel | $K_1$ SDAS | $K_2$ Excel | $K_2$ SDAS |
|-------------|-------------|------------|-------------|------------|
| 17          | 217         | 217        | 1465        | 1467       |
| 24          | 237         | 237        | 1279        | 1279       |
| 35          | 401         | 400        | 525         | 562        |
| 44          | 206         | 206        | 775         | 776        |

*Note: Because both programs gave the same results, only Excel was used for the remainder of the work.*

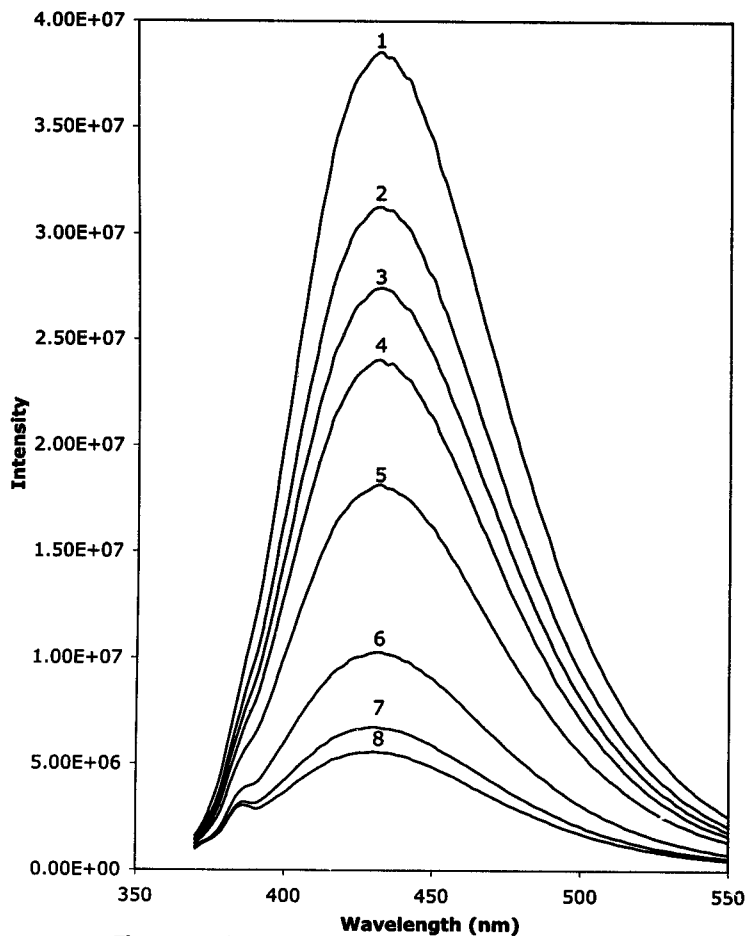


**Figure 7.** Fluorescence spectrum of 2-AN with TM- $\alpha$ -CD. TM- $\alpha$ -CD concentrations: (1) 0, (2)  $5.00 \times 10^{-4}$ , (3)  $7.50 \times 10^{-4}$ , (4)  $1.00 \times 10^{-3}$ , (5)  $1.50 \times 10^{-3}$ , (6)  $2.50 \times 10^{-3}$ , (7)  $3.50 \times 10^{-3}$ , (8)  $4.00 \times 10^{-3}$

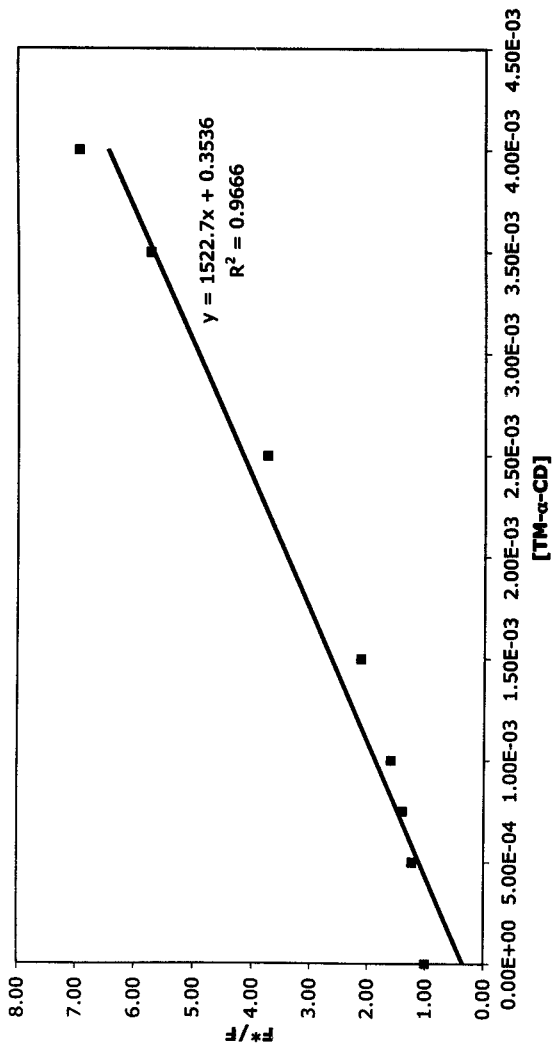


Figure 8. Stern-Volmer Plot of 2-AN with TM- $\alpha$ -CD at 24 C

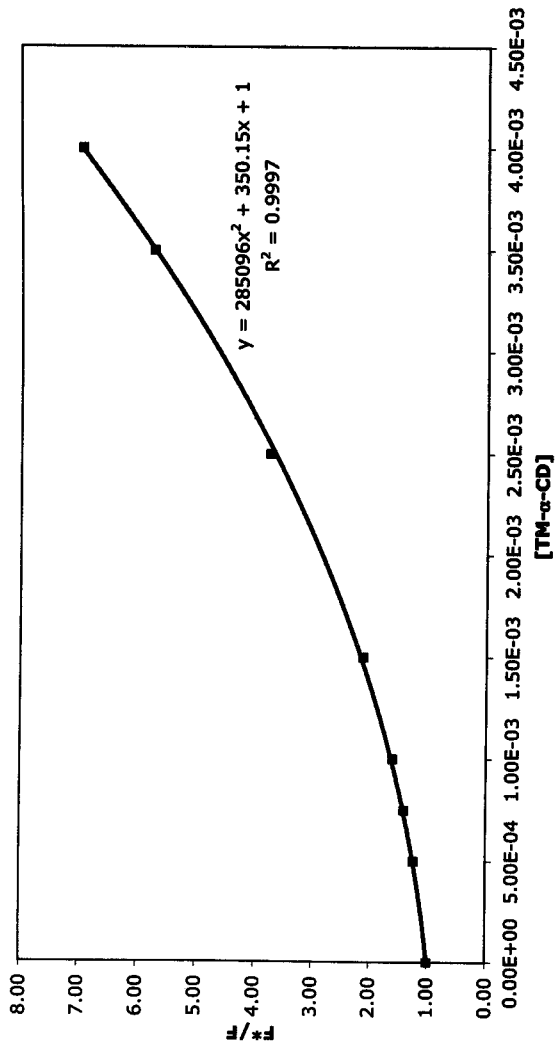


Figure 9. Stern-Volmer Plot of 2-AN with TM-α-CD at 24 C



$$y = 1 + K*x + K*J*x^2$$

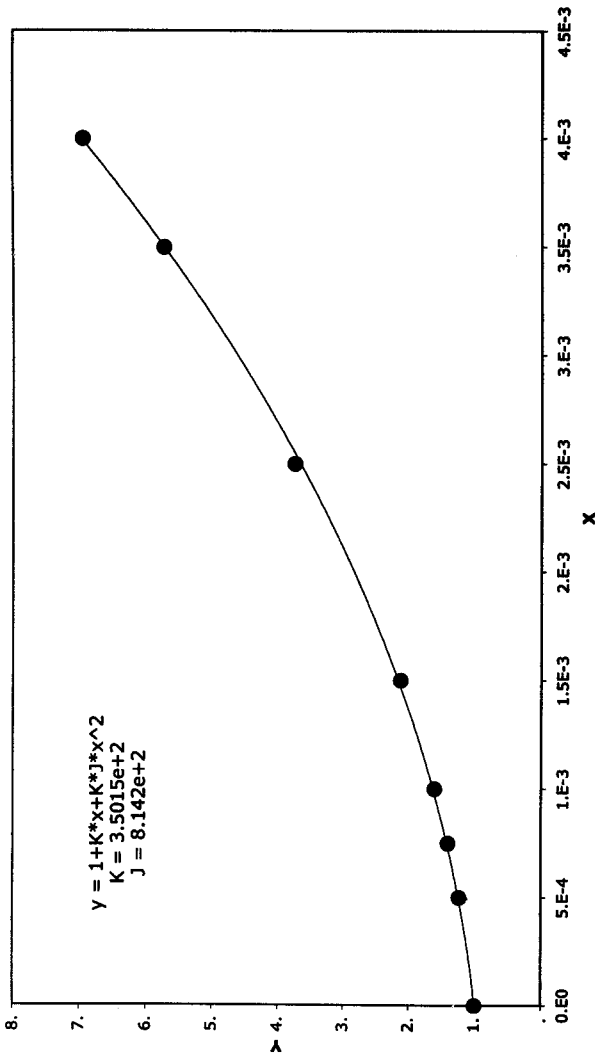


Figure 10. 2-AN with TM- $\alpha$ -CD fit with SDAS at 24C

**Binding of 2-AN with a Fixed Concentration TM- $\alpha$ -CD and Varying Concentrations of  $\alpha$ -CD**

The fluorescence spectra collected for 2-AN with a fixed concentration of TM- $\alpha$ -CD and varying concentrations of  $\alpha$ -CD were similar to those of Figure 4. The modified Stern-Volmer plots did not show the upward curvature that was seen with only TM- $\alpha$ -CD; instead they were linear (see Figure 11).

It was also observed that the K value decreased in the presence of TM- $\alpha$ -CD. For  $\alpha$ -CD alone, the average binding constant from the two trials was  $35 \pm 1$ . When combined with TM- $\alpha$ -CD the average K value decreased to  $24 \pm 2$ . In addition, the quenching of the 2-AN fluorescence with  $\alpha$ -CD and TM- $\alpha$ -CD is significantly less than the quenching of 2-AN with TM- $\alpha$ -CD alone. The quenching observed for 2-AN with  $\alpha$ -CD alone is also less than that of 2-AN with TM- $\alpha$ -CD (see Figure 12).

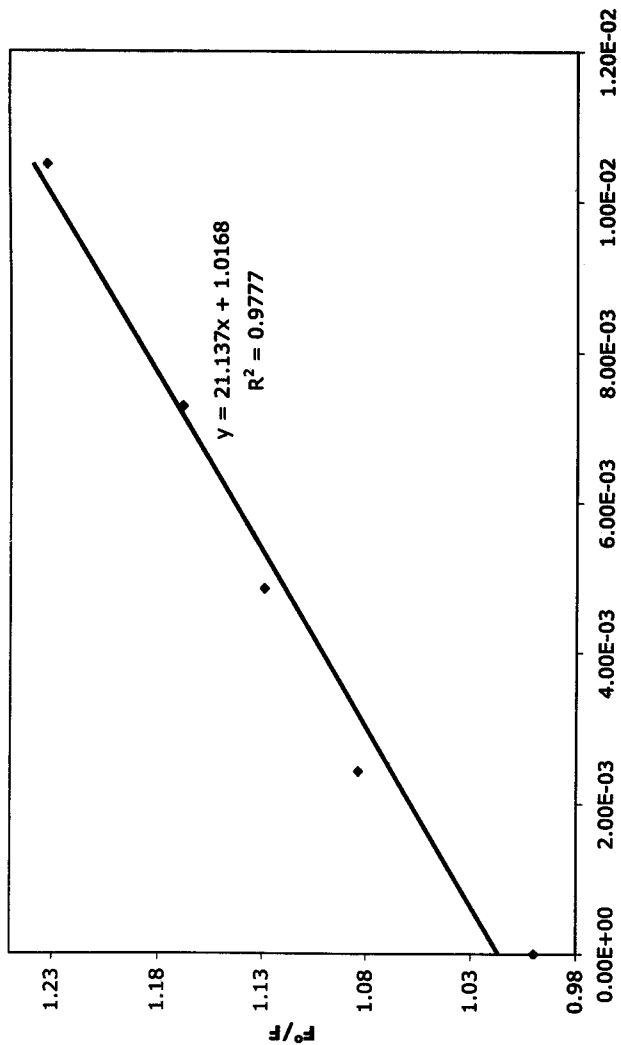


Figure 11. Modified Stern-Volmer plot of 2-AN with TM- $\alpha$ -CD and  $\alpha$ -CD

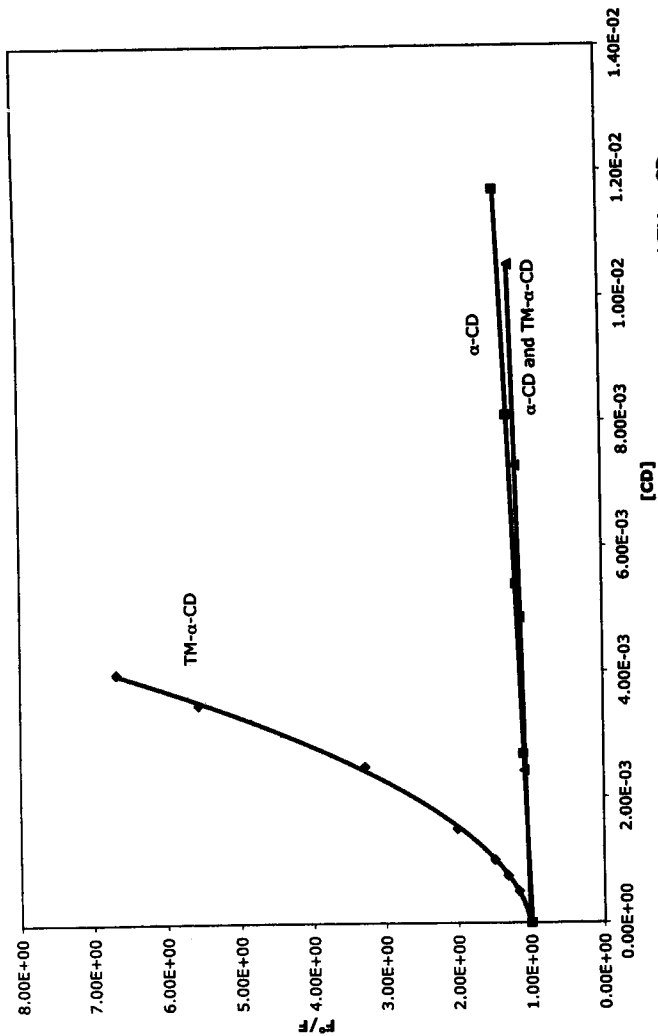


Figure 12. Quenching data for 2-AN with TM- $\alpha$ -CD,  $\alpha$ -CD,  $\alpha$ -CD and TM- $\alpha$ -CD

**The Fluorescence Intensity of 2-AN in the Presence of TM- $\gamma$ -CD**

Figure 13 is an example of a fluorescence quenching spectra for 2-AN with TM- $\gamma$ -CD. In all cases there was little to no change in the fluorescence intensity as the concentration of the cyclodextrin was varied.

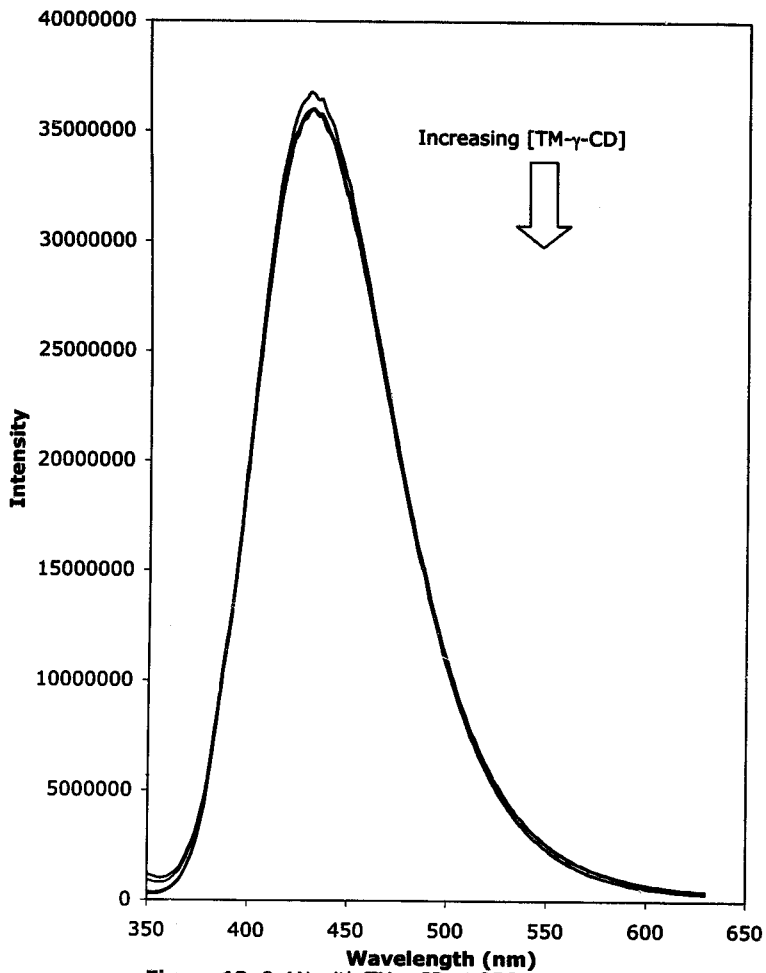


Figure 13. 2-AN with TM- $\gamma$ -CD at 25C

### The Binding of 2-AN to TM- $\alpha$ -CD and DM- $\beta$ -CD

The results of fluorescence intensity measurements of 2-AN binding to TM- $\alpha$ -CD and DM- $\beta$ -CD produced spectra similar to the in Figure 1. For all three trials the temperature was constant at 25 °C. As expected, the fluorescence intensity decreased with the increase of cyclodextrin concentration.

Binding constants were obtained for these data using a modified Stern-Volmer equation. The results are summarized in Table 12.

Table 12. 2-AN with TM- $\alpha$ -CD and DM- $\beta$ -CD data summary

| Trial # | K    |
|---------|------|
| 1       | 1604 |
| 2       | 1483 |
| 3       | 1372 |

### The Binding of 2-AN to TM- $\beta$ -CD and DM- $\beta$ -CD

The results of fluorescence intensity measurements of 2-AN binding to TM- $\beta$ -CD and DM- $\beta$ -CD produced spectra similar to the in Figure 1. As the concentration of cyclodextrin increased, the fluorescence intensity decreased. Binding constants were determined using a modified Stern-Volmer equation. Table 13 summarizes the data obtained.

Table 13. 2-AN with TM- $\alpha$ -CD and DM- $\beta$ -CD data summary

| Trial # | K    |
|---------|------|
| 1       | 1148 |
| 2       | 1081 |
| 3       | 1048 |

## DISCUSSION

Previous researchers have measured the binding constants of both native and methylated cyclodextrins. In this work we further expanded on this list of K values in addition to comparing and contrasting our values with the literature values. Table 14 is a summary of all the binding constants considered in this work.

**Table 14. Summary of Binding Constants for Native and Methylated CD's**

| Cyclodextrin                       | Binding Constant (K) |
|------------------------------------|----------------------|
| $\alpha$ -CD <sup>7</sup>          | 38 +/-5              |
| TM- $\alpha$ -CD (K <sub>1</sub> ) | 209 +/-79            |
| TM- $\alpha$ -CD (K <sub>2</sub> ) | 1273 +/-429          |
| $\beta$ -CD <sup>7</sup>           | 581 +/-6             |
| DM- $\beta$ -CD                    | 918 +/-18            |
| TM- $\beta$ -CD <sup>2</sup>       | 101 +/-4             |
| $\gamma$ -CD <sup>7</sup>          | 49 +/-15             |
| TM- $\gamma$ -CD                   | None                 |

### A. The Binding of 2-AN with DM- $\beta$ -CD

Previous work shows that the binding constants of 2-AN with  $\beta$ -CD and TM- $\beta$ -CD at 25 °C are 581 +/-6 and 101 +/-4, respectively<sup>1,7</sup>. In this work we found that the 2-AN and DM- $\beta$ -CD complex has a binding constant of 918 +/-18 at 25 °C. When 2-AN binds with  $\beta$ -CD, it is likely that not all of the 2-AN enters the hydrophobic cavity; rather, the less hydrophobic portion sticks out of the cavity. However, when a cyclodextrin is methylated the hydrophobic cavity is extended, therefore increasing the surface area available for binding and the amount of 2-AN physically in the cavity. Because the 2-AN is able to bind to a greater area of the cyclodextrin, the binding is stronger than that with the  $\beta$ -CD, where the hydrophobic cavity is smaller.

The thermodynamic data calculated for the 2-AN:DM- $\beta$ -CD complex also implies that greater contact between the 2-AN and the CD due to the extended hydrophobic



cavity is possible. For unsubstituted  $\beta$ -CD  $\Delta H^\circ$  has been measured as  $-11.9$  kJ/mol and  $\Delta S^\circ$  as  $12.5$  J/mol. The large negative  $\Delta H^\circ$  ( $-19.5 \pm 1.8$  kJ/mol) for DM- $\beta$ -CD indicates a stronger host:guest interaction and the large negative  $\Delta S^\circ$  ( $-9.3 \pm 5.9$  J/mol) is consistent with a more restricted orientation and therefore a more rigid environment. Therefore, the thermodynamic data are consistent with the binding constant data.

When the  $\beta$ -CD is fully methylated, it has been shown that, unlike DM- $\beta$ -CD, the integrity of the hydrophobic cavity is lost<sup>8</sup>. The hydrogen bonding present between the -OH groups of the native cyclodextrins plays a role in the stabilization of their torroidal shape; the complete loss of this hydrogen bonding may lead to significant distortion of this shape. This has been shown through both NMR and molecular modeling studies<sup>3-6</sup>. The low binding between 2-AN and TM- $\beta$ -CD can be explained by this distortion, which does not allow the 2-AN molecule to fit as well within the CD cavity and, therefore, strong bonding cannot occur.

#### **B. The Binding of 2-AN with Permethylated Cyclodextrins**

##### **The Fluorescence Intensity of 2-AN in the Presence of TM- $\gamma$ -CD**

Previous work shows that 2-AN and  $\gamma$ -CD have a binding constant of  $49 \pm 5^1$  for the 1:1 complex. This is significantly lower than the other cyclodextrins in this study. However, this can be accounted for by the larger cavity size.  $\gamma$ -CD is composed of eight glucopyranose units and therefore has the largest cavity of the three native cyclodextrins. The binding constant indicates that this cavity size is too big for the 2-AN to bind tightly in the CD cavity. In fact, it appears that, of the native cyclodextrins, 2-AN fits best in the hydrophobic cavity of  $\beta$ -CD (see Table 14).

In this work, we found that, a binding constant cannot be determined when  $\gamma$ -CD is fully methylated. Figure 10 shows that the fluorescence intensity of 2-AN did not change in the presence of TM- $\gamma$ -CD. With both the TM- $\beta$ -CD and the TM- $\gamma$ -CD the binding is significantly reduced when compared to that of the native cyclodextrins (see Table 14). When fully methylated,  $\gamma$ -CD experiences large distortions of its macrocyclic conformation<sup>8</sup>. This large distortion, due to the lack of intramolecular hydrogen bonding, causes the cavity of TM- $\gamma$ -CD to be too small for the 2-AN molecule, greatly reducing the binding constant.

#### The Binding of 2-AN and TM- $\alpha$ -CD

Unlike with other cyclodextrins, the fluorescence data for 2-AN with TM- $\alpha$ -CD did not show linear results when plotted using a modified Stern-Volmer equation (Eq. 1). Rather, the data exhibited obvious upward curvature and were fitted using Eq. 10. In this case, we believe that, in addition to a 1:1 (2-AN:TM- $\alpha$ -CD) complex, a 1:2 (2-AN:(TM- $\alpha$ -CD)<sub>2</sub>) complex is also being formed. The average  $K_1$  value at 25 °C was found to be 209 +/- 79 and the average of  $K_2$  at 25 °C was found to be 1273 +/- 429, where  $K_1$  is for the 1:1 complex, and  $K_2$  is for the 1:2 complex involving two cyclodextrins and one 2-AN molecule.

The formation of the first complex apparently enhances the ease of the second complex formation. This allosteric effect is the reason that  $K_2$  is greater than  $K_1$ . In addition, this implies that there is interaction between the TM- $\alpha$ -CD molecules. This same cooperativity was observed for a range of temperatures. However, the data collected for 25 °C was determined to be the most important because it could be compared to the literature values of the other cyclodextrins.

While the distortion that occurs with TM- $\beta$ -CD does not occur with TM- $\alpha$ -CD to the same degree, Kano and co-workers have shown that TM- $\alpha$ -CD can transform the shape of its cavity to form inclusion complexes. This flexibility has not been shown to occur with the other cyclodextrins in this study and may account for the difference in binding interaction with TM- $\alpha$ -CD (see Table 14).

### C. The Binding of 2-AN in Cyclodextrin Mixtures

Cyclodextrin mixtures were explored in order to determine if mixed binding would occur. For example, we wanted to see if the same 1:2 complex and large quenching would occur in the presence of both TM- $\alpha$ -CD and  $\alpha$ -CD as in the observed with just TM- $\alpha$ -CD alone.

#### Binding of 2-AN with TM- $\alpha$ -CD and $\alpha$ -CD

As can be seen in Figure 8, the combination of 2-AN with  $\alpha$ -CD and TM- $\alpha$ -CD did not yield the same upward curvature that TM- $\alpha$ -CD alone gave. In addition, the amount of quenching significantly decreased when the two were combined (see Figure 9). It should be noted, that, in Figure 9, even though it appears that the lines for  $\alpha$ -CD alone and the mixture of the two CD's are flat, they do increase linearly. The significantly large quenching for TM- $\alpha$ -CD merely flattens the other two lines. This implies that a 1:2 complex like that which forms between 2-AN and TM- $\alpha$ -CD, does not form in the presence of  $\alpha$ -CD and TM- $\alpha$ -CD.

The presence of TM- $\alpha$ -CD leads to an apparent drop in K (from 35 +/- 1 to 24 +/- 2) for the  $\alpha$ -CD:2-AN complex. From this observation we can infer that there is an interaction between the TM- $\alpha$ -CD and the  $\alpha$ -CD. This interaction would lead to a decrease in the equilibrium concentration of  $\alpha$ -CD. Therefore, the assumption that the

equilibrium concentration is the analytical concentration is inaccurate leading to the apparent decrease in  $K$  for the  $\alpha$ -CD:2-AN complex.

**The Binding of 2-AN with TM- $\alpha$ -CD and DM- $\beta$ -CD and 2-AN with TM- $\alpha$ -CD and DM- $\beta$ -CD**

With both of these mixtures, the measured  $K$  values appear to just be the sum of the individual binding constants. This was not further explored because this result suggests no evidence of aggregation between the cyclodextrins.

#### References

1. Werner, T.C., LaRose, J.H., *Appl. Spec.*, **2000**, 54, 2
2. Iannacone, J.M., *The Use of Fluorescence to Investigate the Factors Leading to Complex Formation Between Naphthalenes and  $\beta$ -Cyclodextrins*, **2003**, Union College Senior Thesis
3. Ucello-Barretta, G., Balzano, F., Cuzzola, A., Menicagli, R, Salvadori, P., *Eur. J. Org. Chem.*, **2000**, 449-453
4. Kojikano, Ishimura, T., Negi, S., *Journal of Inclusion Phenomena and Molecular Recognition in Chemistry*, **1995**, 22, 285-298
5. Reinhardt, R., richter, M., Mager, P., *Carbohydrate Research*, **1996**, 291, 1-9
6. Schneider, H., Hacket, F., Rudiger, V., *Chem. Rev.*, **1998**, 1755-1785
7. Fraiji, E.K., Cregan, T.R., Werner, T.C., *Applied Spectroscopy*, **48**, **1994**, 1
8. Botsi, A., Yannakopoulou, K., Hadjoudis, E., *Magnetic Resonance in Chemistry*, **34**, **1996**, 419-423

**Part II.**  
**The use of gas chromatography/mass spectrophotometry to analyze organic contaminants  
in local waters**

## INTRODUCTION

Each year the Quantitative Analysis (Chem. 40) class analyzes local waters for inorganic contaminants using various techniques in a lab known as The Water Project. Recently, the chemistry department obtained a new Agilent Technologies 6891N Gas Chromatograph/ 5973 Mass Spectrophotometer. This new instrument differs from those already in the department because it has an autosampler. The sensitivity of this instrument was expected to be quite high, therefore it seemed appropriate to try and detect organic compounds in water samples. The use of this new instrument would be a facile way to introduce the analysis of organic contaminants into The Water Project.

The main goal of this project was to develop a procedure that could be used in Chem 40 on the water samples collected. The streams used in this project were the Patroon in Albany, NY and the Hans Groot Kill in Schenectady, NY. The Patroon is a relatively polluted, urban stream subject to a significant amount of run off. In addition, the Hans Groot Kill has high counts of *e. coli* and is also subject to run off. Both of these streams had high potential for organic contaminants.

## EXPERIMENTAL

A stock solution containing dodecane, toluene, acetophenone, phenol, and naphthalene was prepared in HPLC grade methanol as described in Table 1.

**Table 1. Preparation of Stock Solution (Total Volume 100mL)**

| Substance    | Volume/Mass Added | [Substance] ppm |
|--------------|-------------------|-----------------|
| Dodecane     | 10 $\mu$ L/7.5mg  | 95              |
| Toluene      | 10 $\mu$ L/8.7mg  | 109             |
| Acetophenone | 10 $\mu$ L/10.3mg | 130             |
| Phenol       | 20.3mg            | 257             |
| Naphthalene  | 14.4 mg           | 182             |

A method was created on the GC/MS and named waterSTD.M. For waterSTD.M the injection was splitless. The column temperature started at 60 °C and remained there for 5 minutes, it then increased by 5 °C per minute to 120 °C, where it remained for 15 minutes.

The stock solution was run using this method (referred to as standard method) with a 1 $\mu$ L and 5 $\mu$ L injection sizes. Serial dilutions of the stock solution were then prepared as described in Table 2.

**Table 2. Serial Dilutions of Stock Solution**

| Volume of Stock | mL of HPLC grade CH <sub>3</sub> OH | Dilution Factor | Solution |
|-----------------|-------------------------------------|-----------------|----------|
| 1 mL            | 1                                   | 1:2             | A        |
| 1 mL            | 4                                   | 1:5             | B        |
| 1 mL            | 9                                   | 1:10            | C        |
| 1 mL            | 19                                  | 1:20            | D        |
| 100 $\mu$ L     | 5                                   | 1:50            | E        |
| 100 $\mu$ L     | 10                                  | 1:100           | F        |

Each solution was run, in triplicate, using the standard method with 1 $\mu$ L, 2 $\mu$ L and 5 $\mu$ L injection sizes. When necessary the peaks were autointegrated. The concentration of each component for all dilutions was calculated and can be seen in Table 3.



**Table 3. Concentration of Each Component in for All Dilutions of Stock Solution**

| Analyte      | (Dilution Factor)Concentration in ppm                    |
|--------------|--|
| Dodecane     | (1:2)48; (1:5)19; (1:10)10; (1:20)5; (1:50)2; (1:100)1   |
| Toluene      | (1:2)55; (1:5)22; (1:10)11; (1:20)6; (1:50)2; (1:100)1   |
| Acetophenone | (1:2)65; (1:5)26; (1:10)13; (1:20)7; (1:50)3; (1:100)    |
| Phenol       | (1:2)129; (1:5)51; (1:10)26; (1:20)13; (1:50)5; (1:100)3 |
| Naphthalene  | (1:2)91; (1:5)36; (1:10)18; (1:20)9; (1:50)4; (1:100)2   |

An average peak height was calculated for samples A-F for the runs with 1 $\mu$ L, 2 $\mu$ L, and 5 $\mu$ L injection sizes. These averages were plotted against analyte concentration.

Both a 1:10 and 1:100 dilutions of F were prepared and run, in triplicate, with the standard method. The concentration of these two dilutions were calculated and can be found in Table 4.

**Table 4. Concentrations of Solution F Dilutions**

| Analyte      | (Dilution Factor)Concentration in ppb |
|--------------|---------------------------------------|
| Toluene      | (1:10)100; (1:100)9.4                 |
| Phenol       | (1:10)100; (1:100)18                  |
| Acetophenone | (1:10)100; (1:100)13                  |
| Naphthalene  | (1:10)300; (1:100)25                  |
| Dodecane     | (1:10)200; (1:100)18                  |

A 1 L, 10 ppm solution of toluene, phenol and acetophenone was then prepared in Millipore water. The organics were then extracted using a Strata-X solid phase extraction disk from Phenomenex. The extraction disk was placed in a vacuum filtration set up and the following were drawn through the apparatus.

1. 1mL of HPLC grade methanol
2. 1mL of Millipore water
3. 1L sample

4. 1mL of 5% HPLC grade methanol in Millipore water

The aspirator vacuum was then allowed to run for about 30 seconds to dry the disk and then the aspirator was removed from the filtration set up. While the disk was drying, a GC/MS sample vial was labeled and the plunger from a sterile 3mL plastic syringe was removed. After drying, the solid phase extraction disk was removed from the filtration set up and 1mL of HPLC grade methanol was pipetted in. The methanol was slowly forced through the extraction disk with the plunger from the 3mL syringe into the GC/MS sample vial. The vial was then capped and run in triplicate with the standard method. Also, a 1L, 2 ppm solution of toluene and acetophenone was prepared in water and run through the same extraction procedure.

An 80 ppb solution was prepared in the following manner. A third stock solution (Stock<sub>3</sub>) was then prepared by measuring 100 $\mu$ L of toluene and 100 $\mu$ L of acetophenone into 1L of Millipore water. In order to reach 80 ppb, 1mL of this solution was diluted in 1L using Millipore water and run through the same extraction procedure. The sample was run, in triplicate, using the standard method. A 500 $\mu$ L aliquot of Stock<sub>3</sub> was also mixed with 1L of Millipore water, sent through the solid phase extraction procedure and run using the same method. In addition, 250 $\mu$ L of Stock<sub>3</sub> were diluted in 1L of Millipore water and

125  $\mu$ L of Stock<sub>3</sub> were diluted in 1L of Millipore water, both were sent through the solid phase extraction procedure and run on the GC using the standard method.

Samples from the Patroon, (total volume 1L) and the Hans Groot Kill (total volume 1L) streams were also sent through the solid phase extraction disk procedure and run, in

triplicate, using the standard method. Both of these water samples were filtered for solid particulates before the solid phase extraction disk procedure was employed.

## RESULTS

The standard method gave five sharp peaks when the stock solution was run, one for each of the analytes (see Figure 1). The order that the components came off the column was toluene, phenol, acetophenone, naphthalene, dodecane. The retention times were 2.788 minutes, 9.281 minutes, 14.121 minutes, 18.905 minutes, and 19.711 minutes respectively. Figure 2 through Figure 6 show the gas chromatogram for the stock solution with the mass spectrum of each peak below. Figures 7 through 11 show the average peak heights (1-6 %RSD) for the dilutions plotted against the analyte concentrations for 1 $\mu$ L, 2 $\mu$ L, and 5 $\mu$ L injection sizes. As the dilution factor became greater, the number of analytes that could be detected decreased. The only analytes that could be detected at the 1:100 dilution were naphthalene and toluene both of which were present at about 1-2 ppm concentrations. As can be seen in Figures 7 through 11, as the injection size increased the peak height also increased.

When Solution F was diluted by a factor of 10 and a factor of 100 all of the components were present in concentrations less than 1 ppm (see Table 4). Neither of the solutions had detectable amounts of the analytes.

The 10 ppm solution of toluene, phenol, and acetophenone and 2 ppm solution of toluene and acetophenone both gave sharp peaks for toluene (2.77 minute retention time) and acetophenone (14.15 minute retention time) (see Figures 12 and 13). From the 10 ppm solution it was found that phenol would not be detected at low concentrations even when put through the solid phase extraction disk. Therefore, solutions of only toluene and acetophenone were prepared.

The 80 ppb and 40 ppb solutions of toluene and acetophenone gave sharp peaks for both analytes ( see Figures 14 and 15). The extraction efficiency was calculated to be about 70% for both analytes in the 80 ppb solution and 10% for toluene and 30% for acetophenone in the 40 ppb solution. The 20 ppb and 10 ppb solutions also gave sharp peaks for both analytes however, the chromatograms were starting to become more noisy, autointegration was necessary to detect toluene and the data were not as reproducible as the higher concentrations. The average extraction efficiency is about 25% for toluene and >100% for the acetophenone in the 20 ppb solution. For the 10 ppb solution the extraction efficiency was calculated to be 15% for toluene and 70% for acetophenone.

The Patroon sample did not have detectable amounts of the five analytes being studied here. It did, however, have a significant amount of diethyl phthalate. This sample was run in triplicate, the first chromatogram was extremely noisy (Figure 16). The remaining two had several small peaks, but the diethyl phthalate peak (25.52 minute retention time) was significantly larger than the rest (Figure 17). This was confirmed by running a known solution of diethyl phthalate in methanol and seeing a similar peak at 25.6 minutes. The Hans Groot Kill gave similar results. The first run was extremely noisy and looked very similar to Figure 17. However, the second and third run gave large, slightly broad peaks that were identified as 2-acetylnaphthalene (Figure 18).

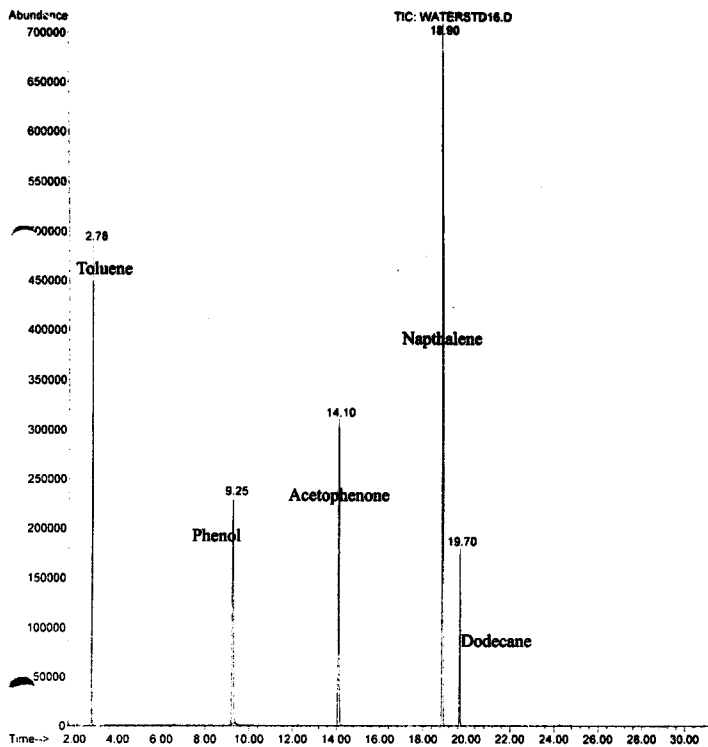
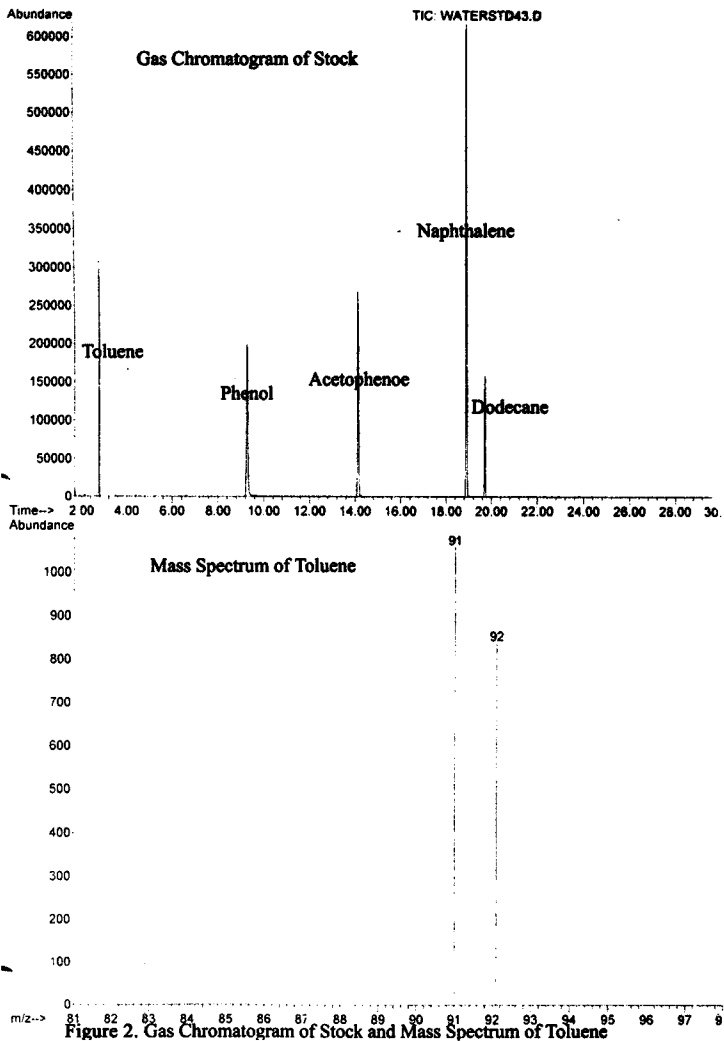


Figure 1. Gas Chromatogram of Stock



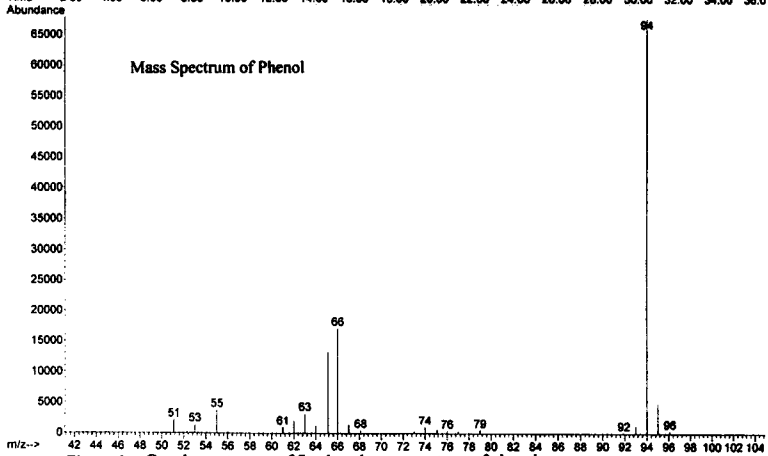
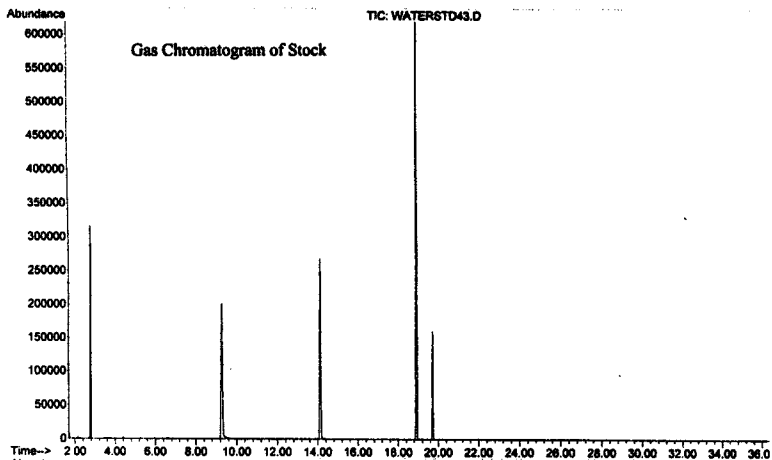


Figure 3. Gas chromatogram of Stock and mass spectrum of phenol



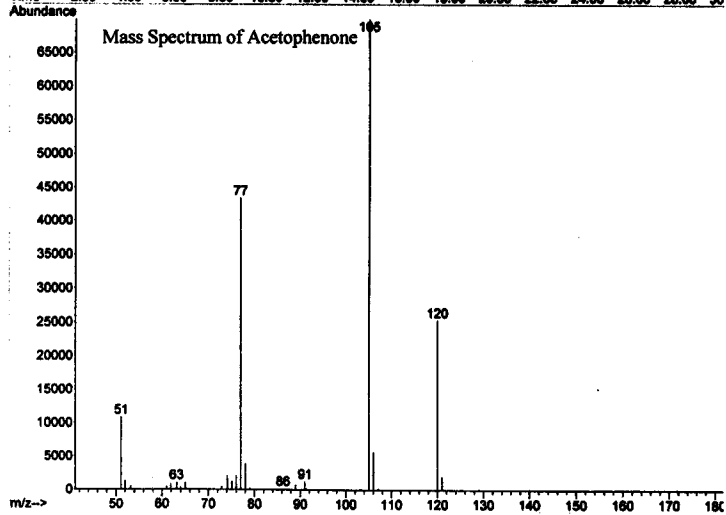
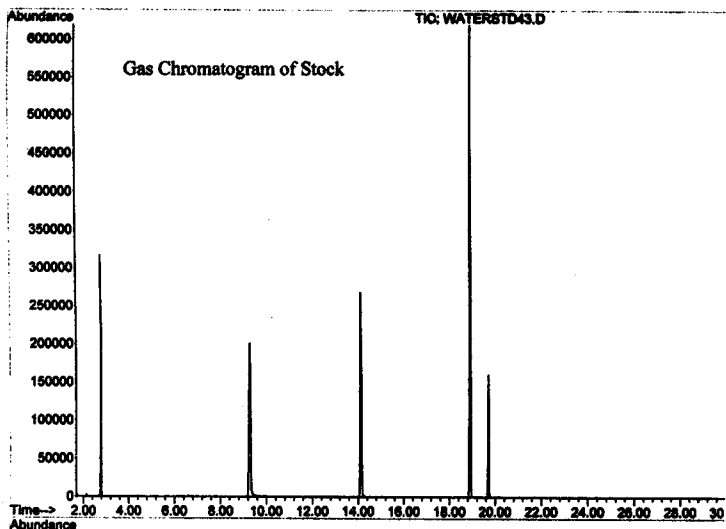


Figure 4. Gas chromatogram of Stock and mass spectrum of acetophenone

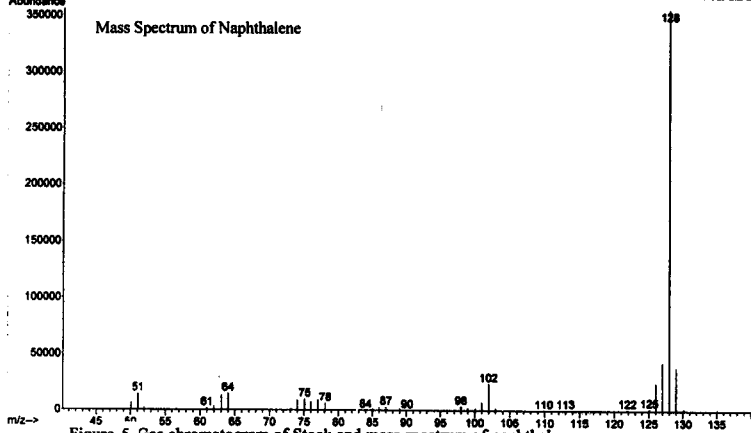
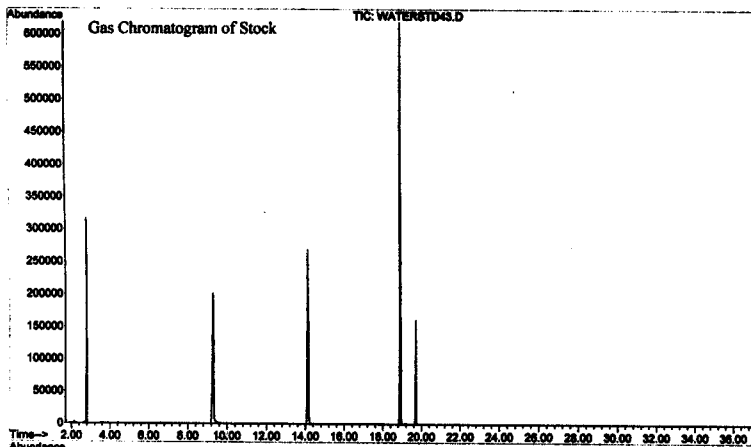


Figure 5 Gas chromatogram of Stock and mass spectrum of naphthalene

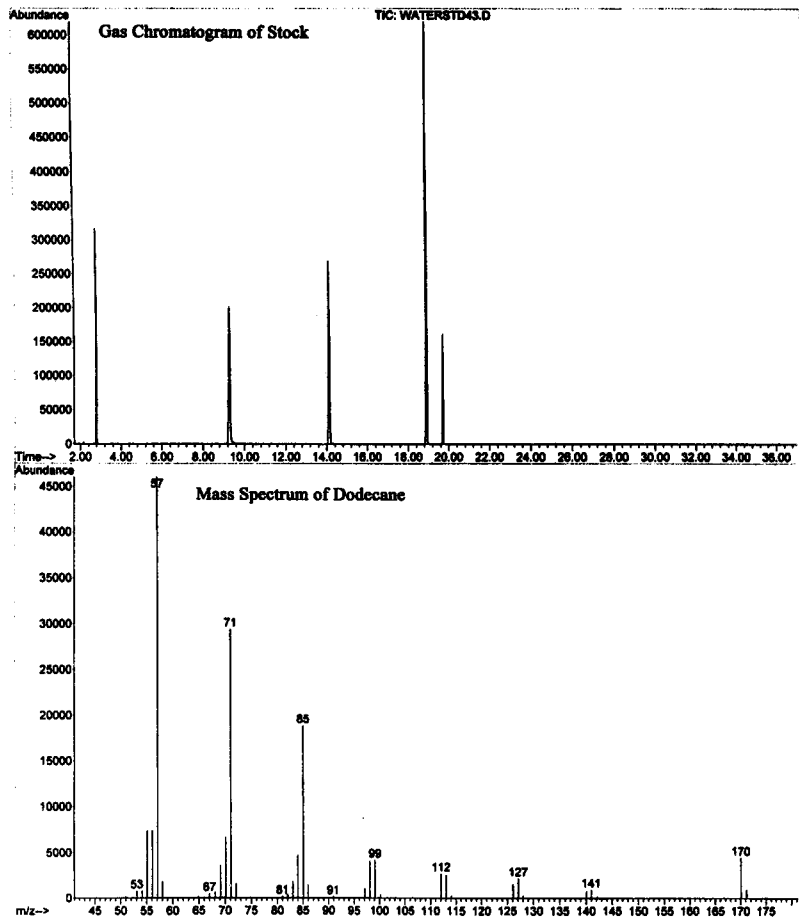


Figure 6. Gas chromatogram of stock and mass spectrum of dodecane

UN82 PAYEUR, AMY L. BINDING STUDIES OF 2-ACETYLNAPHTHALENE ETC  
P343b/2004 CHEMISTRY HRS. 6/04 2-2



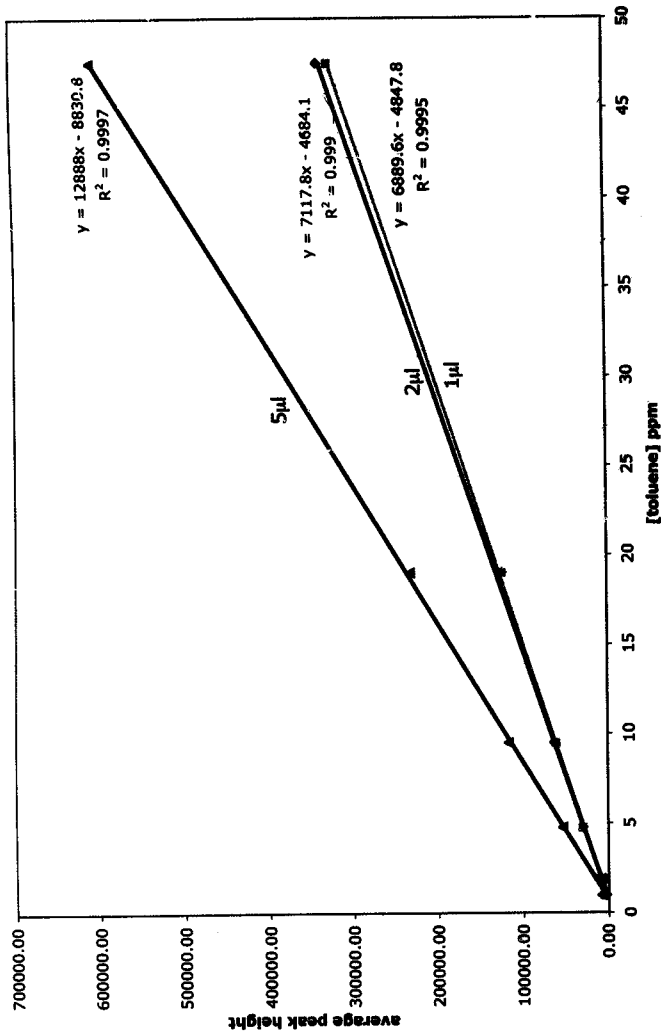


Figure 7. Average peak heights vs. toluene concentration for 1μL, 2μL and 5μL Injection sizes

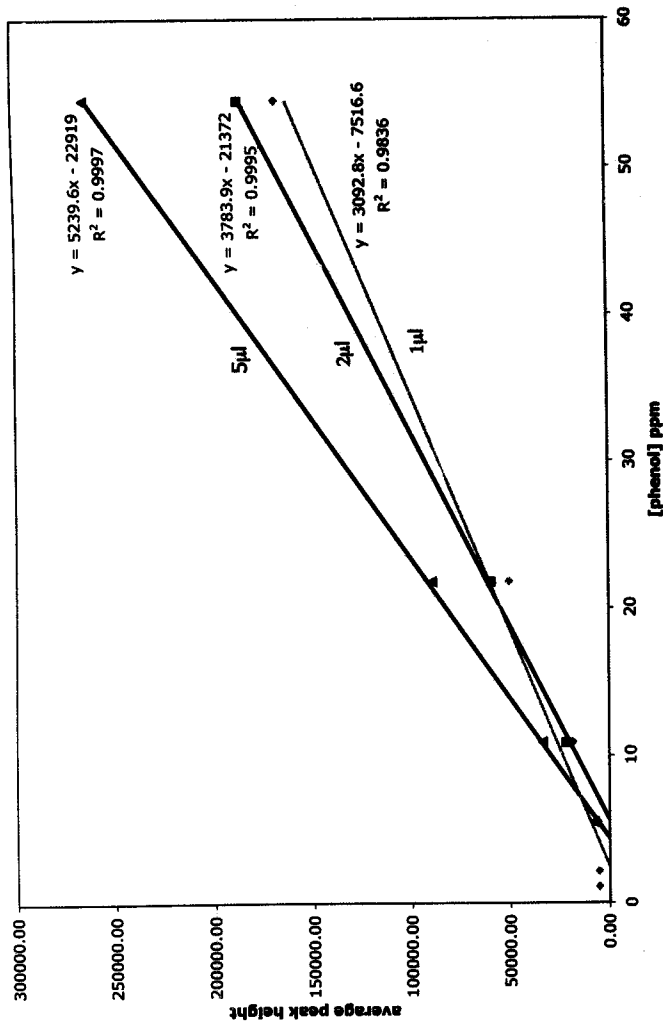


Figure 8. Average peak heights vs. phenol concentration for 1µL, 2µL and 5µL injection sizes

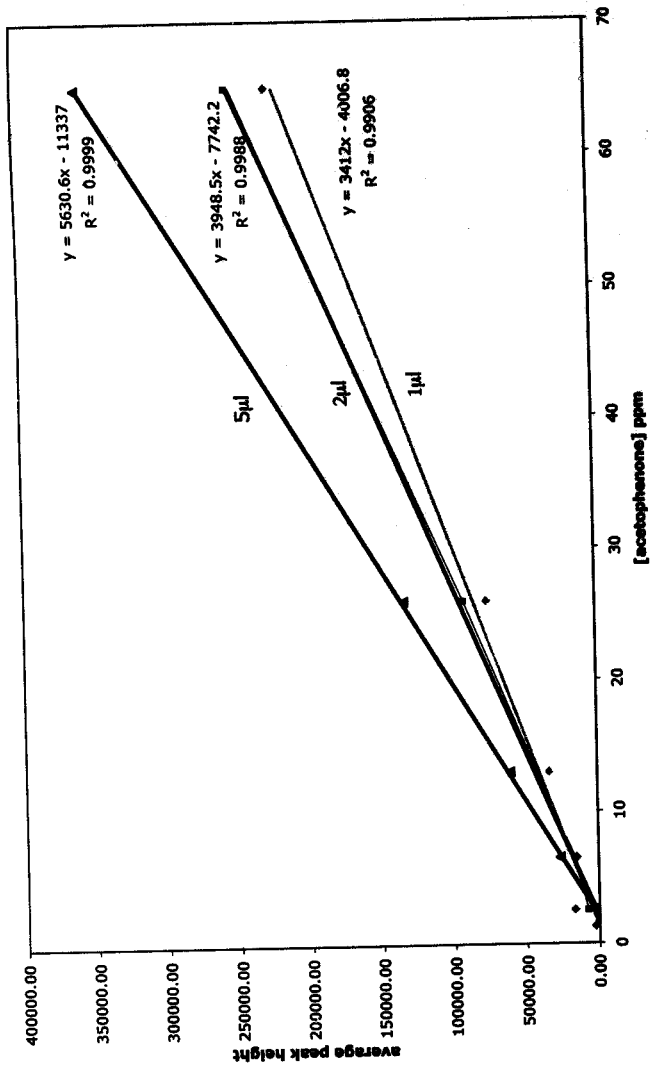


Figure 9. Average peak heights vs. acetophenone concentration for 1µl, 2µl and 5µl injection sizes

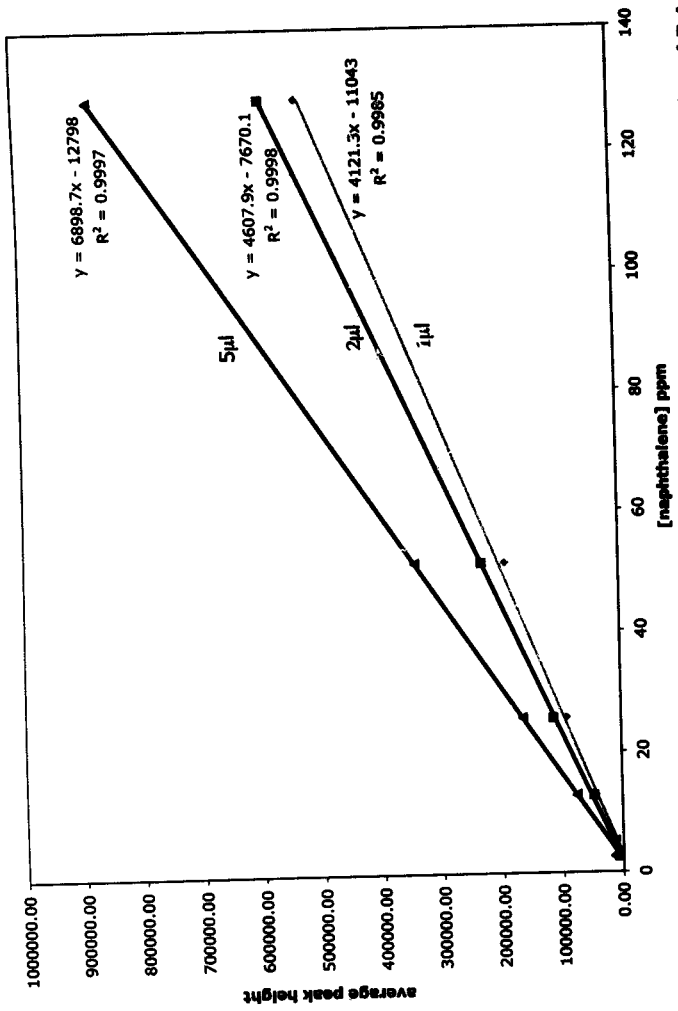


Figure 10. Average peak heights vs. naphthalene concentration for 1µl, 2µl, and 5µl infection sizes



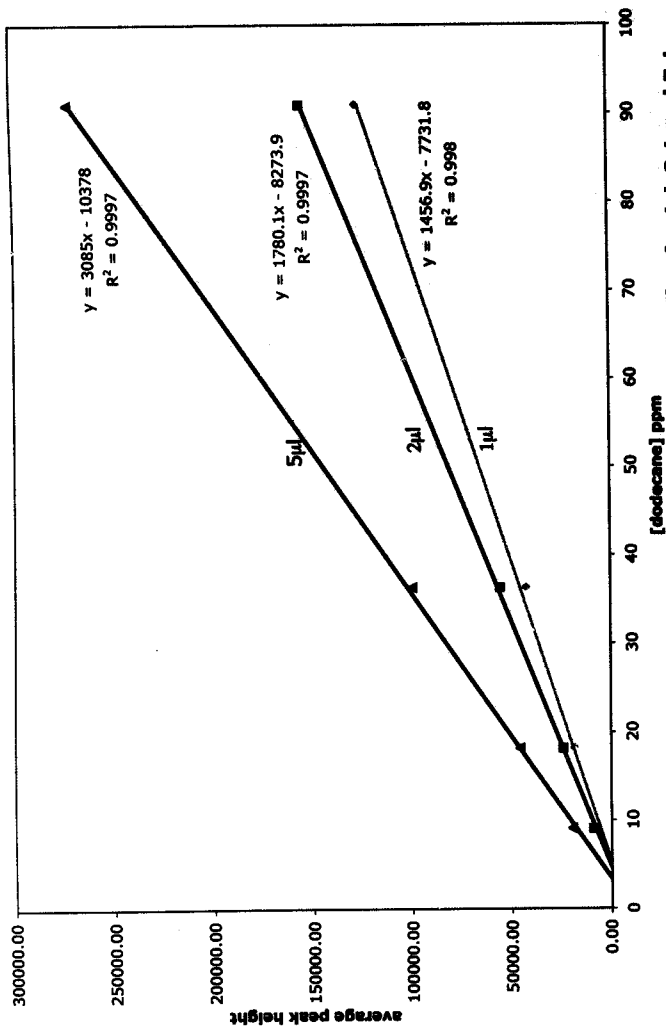


Figure 11. Average peak heights vs. dodecane concentration for 1µl, 2µl and 5µl infection sizes

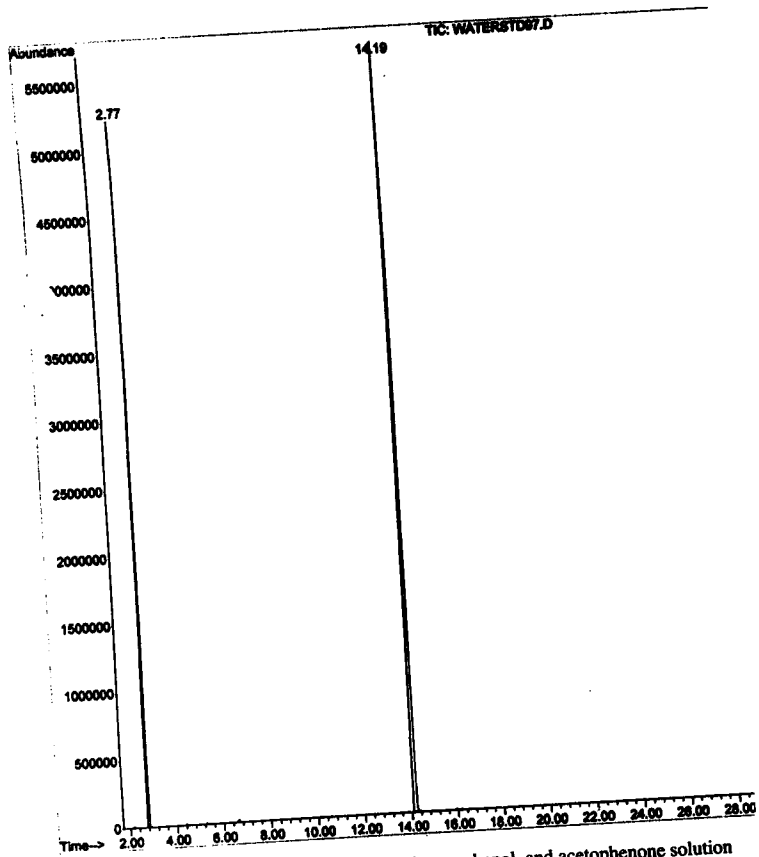


Figure 12. Gas chromatogram of 10 ppm toluene, phenol, and acetophenone solution

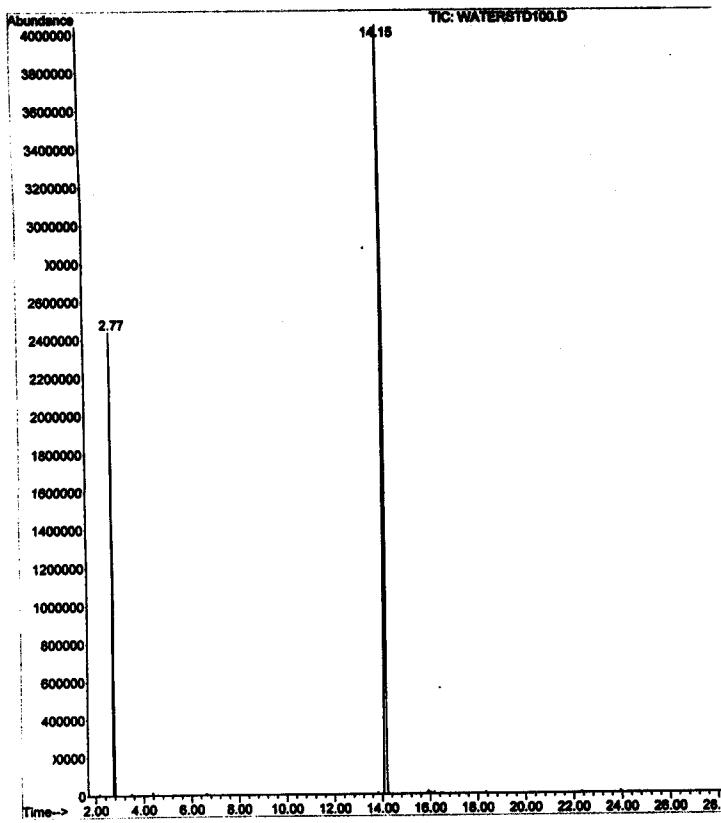


Figure 13. Gas chromatogram of 2 ppm toluene and acetophenone solution

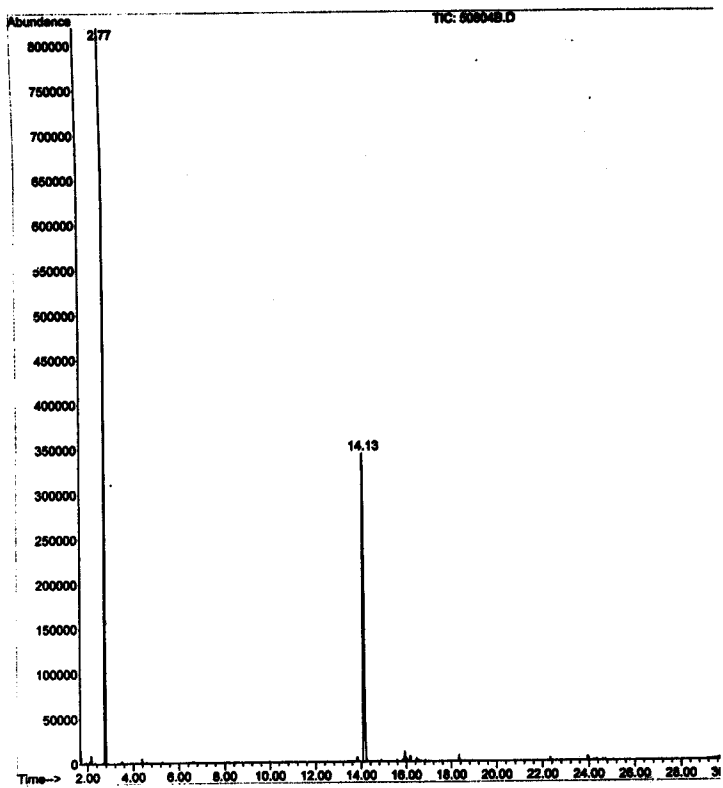


Figure 14. Gas chromatogram of solutions with 80 ppb toluene and acetophenone

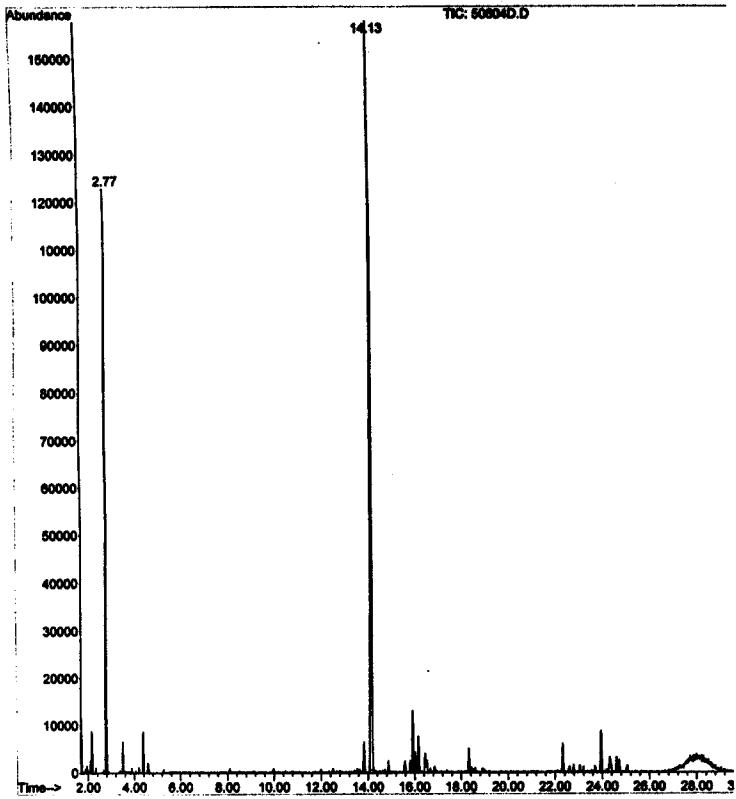


Figure 15. Gas Chromatogram of 40 ppb toluene and acetophenone solution

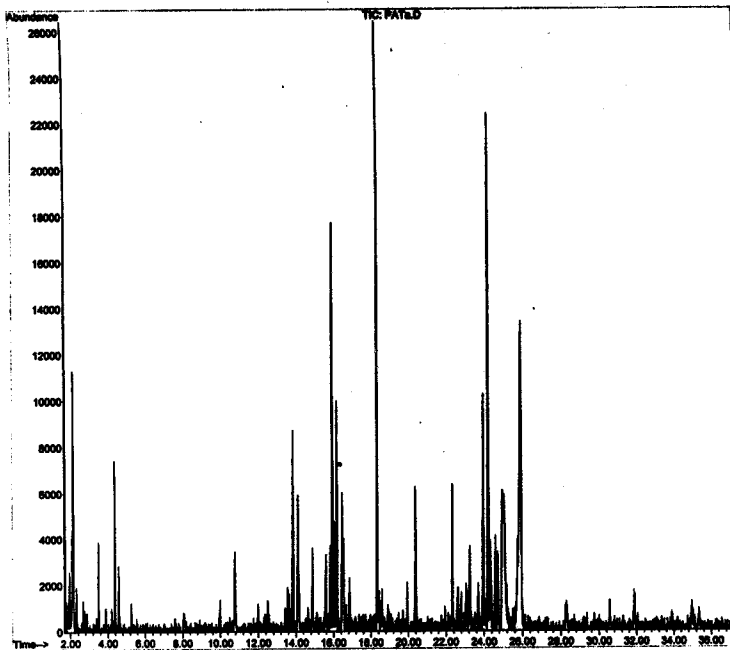


Figure 16. Gas chromatogram of Patroon sample, run 1.

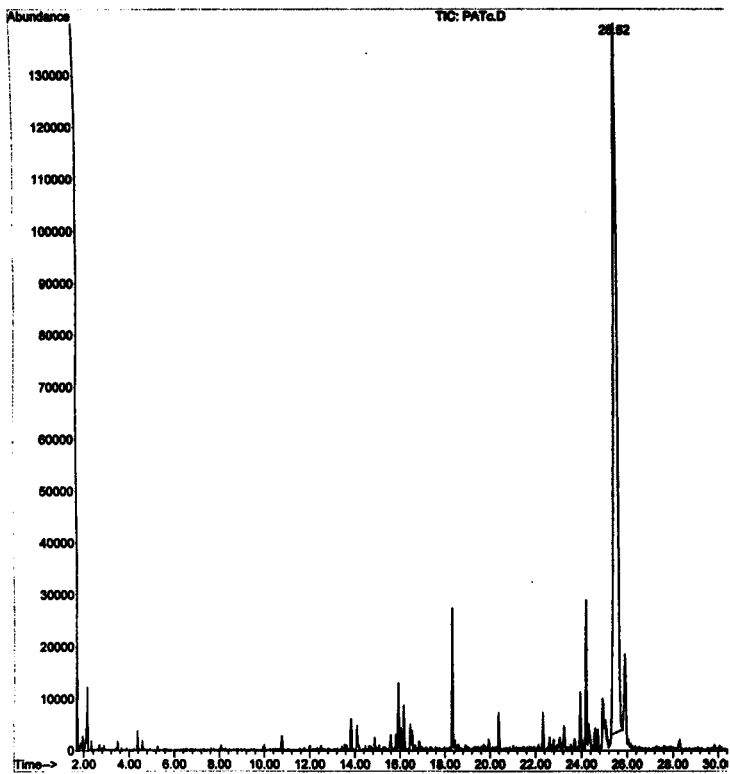


Figure 17. Gas Chromatogram of the Patroon sample

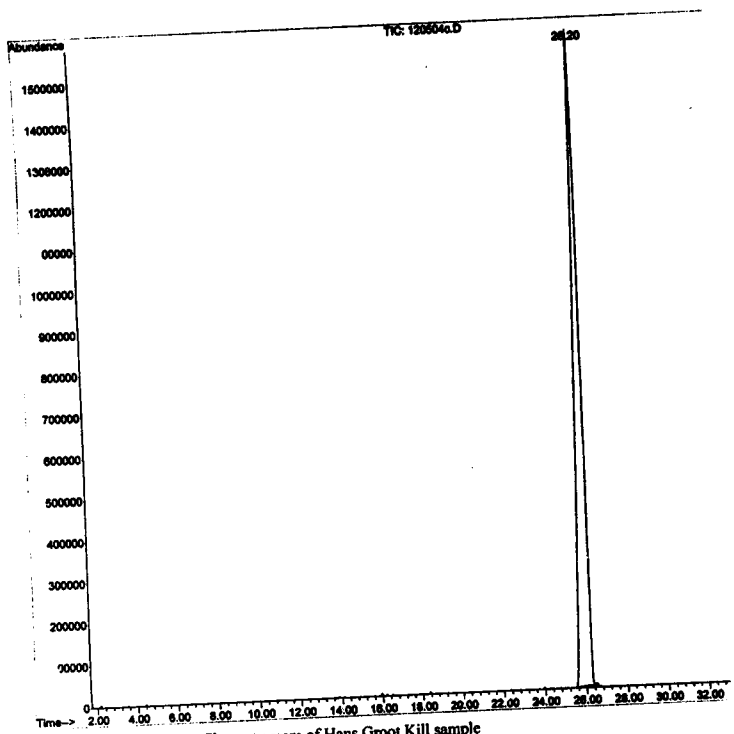


Figure 18. Gas Chromatogram of Hans Groot Kill sample



## DISCUSSION

The parameters for the standard method were selected because all five peaks were present and sharp. In addition, it was believed that this method would be suitable for running water samples which include a range of organics not in the Stock. The limit of detection for the organic analytes with the standard method was determined to be about 1 ppm. The data collected from the Stock and the dilutions of the Stock make this clear. Below 1 ppm no analytes were detected; however, at the 1 ppm concentration two of that analytes, toluene and naphthalene, were detected. A 5  $\mu\text{L}$  injection size was determined to be ideal because, as can be seen in Figures 7 through 11, larger injection sizes provided higher peaks. As would be expected, in the 5  $\mu\text{L}$  injections, more material is being injected into the column and therefore it is more easily detected. A 10  $\mu\text{L}$  injection size was explored, however an injection of this size is not possible with the syringe currently in the instrument.

It is known that in water systems organic contaminants are present in concentrations below the ppm level. Therefore, in order to employ this method in The Water Project a preconcentration step is necessary; this lead to the development of the use of the solid phase extraction disk. Only toluene, phenol and acetophenone were dissolved in water to test this method because naphthalene and dodecane are too hydrophobic to ensure adequate water solubility. When the first solution was run, only toluene and acetophenone were detected. This may be because the phenol was either bound tightly to the solid phase extraction disk and was not eluted by the methanol or it was not bound at all and remained in the water. This result lead to the decision to use only toluene and acetophenone in the solutions.

Toluene and acetophenone were detectable using the solid phase extraction disk, at concentrations as low as 10 ppb. However, the reproducibility decreased as the concentrations decreased. The 80 ppb solution had an extraction efficiency of 70% for both analytes, indicating that the solid phase extraction disk procedure is quite successful in this concentration range. However, for 40 ppb it dropped significantly and below that the extraction efficiency became undesirable. In fact, the extraction efficiency was greater than 100% for acetophenone in the 20 ppb solution. The inconsistencies in the extraction efficiencies may be due to the volumes of methanol actually eluting through the disk, often less than 1 mL made it through the disk and into the vial, some always remained on the disk. Also, it is possible that at concentrations this low the extraction disk is interfering with the analyte concentrations and causing the data to be erroneous.

The solid phase extraction disk combined with the GC method was found to be quite successful for both samples run from actual water systems. Diethyl phthalate was detected in the Patroon which, based on the streams location, seem extremely realistic. Diethyl phthalate is a synthetic substance commonly used to make plastics more flexible. It is found in toothbrushes, toys, tools, automobile parts, food packaging, cosmetics, insecticides and aspirin. These products release diethyl phthalate fairly easily because it is not part of their polymer chain composition. Water sources, like the Patroon, can be contaminated by run off from waste sites and landfills that contain discarded plastics<sup>1</sup>.

The Hans Groot Kill was found to have high concentrations of 2-acetylnaphthalene (2-AN). This was a less expected result than that of the Patroon because 2-AN is not a common contaminant in water systems and no information is available on possible sources.

### References

1. Werner, T.C., LaRose, J.H., *Appl. Spec.*, **2000**, *54*, 2
2. Iannacone, J.M., *The Use of Fluorescence to Investigate the Factors Leading to Complex Formation Between Naphthalenes and  $\beta$ -Cyclodextrins*, **2003**, Union College Senior Thesis
3. Ucello-Barretta, G., Balzano, F., Cuzzola, A., Menicagli, R, Salvadori, P., *Eur. J. Org. Chem.*, **2000**, 449-453
4. Kojikano, Ishimura, T., Negi, S., *Journal of Inclusion Phenomena and Molecular Recognition in Chemistry*, **1995**, *22*, 285-298
5. Reinhardt, R., richter, M., Mager, P., *Carbohydrate Research*, **1996**, *291*, 1-9
6. Schneider, H., Hacket, F., Rudiger, P., *Int. Chem. Rev.*, **1998**, 1755-1785
7. Fraiji, E.K., Cregan, T.R., *Journal of Applied Spectroscopy*, **48**, **1994**, 1
8. Botsi, A., Yannakopoulou, K., Hadjoudis, E., *Magnetic Resonance in Chemistry*, **34**, **1996**, 419-423